현생 조간대 탄성파탐사 기법 정립과 한반도 남·서해안 현생 조간대 퇴적체의 퇴적모델 및 분류 기획 연구

Seismic survey on modern tidal-flat environments and classification/sedimentary model of tidal-flat environments along the southern and western Korean Peninsula

2009년 7월

한국해양연구원

제 출 문

한국해양연구원장 귀하

본 보고서를 '한국해양연구원 2008년도 개인창의과제'의 최종보고서로 제출합니다.

2009년 7월

연구책임자: 이상훈

참여연구원: 김한준, 주형태, 박영길

목 차

1. 추진 필요성 및 목적

1.1. 추진 필요성

□ 한반도 남·서해안에 광범위하게 분포하는 현생 조간대 퇴적체는 육지와 연안해양환경을 연결하는 시스템으로 조간대 퇴적체의 발달 양상과 분류 연구는 장기적인 육지와 연안해양환경의 상호작용을 이해하고 생태계 이해와 보존, 연안 개발과 보전을 하는데 필수적임

□ 현생 조간대 퇴적체는 마지막 해수면 상승시기 동안 공급되는 퇴적물 종류, 퇴적물 이동 양상, 해양작용, 고지형 등 많은 요인들에 의해 다양한 발달 양상을 보이는데 한반도 남·서해안 현생 조간대 퇴적체의 특징과 발달양상을 규명한 연구가 미비하고 이를 통한 조간대 퇴적체의 분류가 전혀 이루어지 않음

□ 2007년 태안해역에서 발생한 유류유출 사고 때 유출된 유류가 조간대에 도달하고 조간대 퇴적체(퇴적층)내로 유입되면서 저서생태계 파괴와 퇴적물 오염을 일으킴. 일반적으로 조간대 퇴적체에 유입된 유류는 조간대 퇴적체의 구성물질, 퇴적형태, 등에 따라 이동 및 집적이 결정됨. 따라서 한반도 남·서해안에 분포하는 현생 조간대 퇴적체의 특징, 발달 양상 및 분류 연구는 향후 유류 유출사고에 따른 조간대 해안의 유류오염을 효과적으로 방제하고 복원하는데 매우 중요함

□ 한반도 남·서해안 현생 조간대 퇴적체의 특징, 발달 양상 및 분류 연구를 위해서는 조간대에서 탄성파탐사 기법이 반드시 필요함

□ 해양환경에서 해저퇴적체(또는 퇴적층)의 특성들을 파악하는데 탄성파탐사 기법이 매우 자주 이용됨. 하지만 현생 조간대 환경은 주기적으로 대기에 노출되고 수심이 매우 얕기 때문에 해양 탄성파탐사 기법을 적용하기 매우 어려움.

□ 현생 조간대 환경에서 해양 탄성파탐사 기법을 적용하기 어렵기 때문에 현재까지는 표층퇴적물, 표층 지형 및 길이가 짧은 캔코어 퇴적물과 간혹 고비용의 시추퇴적물을 이용하여 조간대 퇴적체에 대한 연구를 해왔음.

□ 최근 석유 가격이 급등하면서 오일샌드(oil sand)에 대한 관심이 높아지고 오일샌드의 생산량이 증가하고 있음. 현재 생산되는 오일샌드는 주로 조간대 퇴적층(퇴적체)에 분포하고 있어서 Exxon Mobil, BP 및 Shell과 같은 대형 외국석유회사들은 조간대 퇴적체의 지형, 발달 형태, 발달과정 및 퇴적 모델에 관한 연구에 많은 비용을 투자하고 있음. 이러한 연구는 주로 고기(ancient) 조간대 퇴적층에 이루어졌지만 최근에 현생(modern) 조간대 퇴적체에서 연구가 활발해지고 있음. 이로 인해 현생 조간대 퇴적체에서 탄성파 탐사 기법 연구가 초기 단계에서 활발하게 진행 중임. 우리나라 서해안 및 남해안 지역에서는 현생 조간대 퇴적체가 광범위하게 분포하고 있기 때문에 현생 조간대 퇴적체에서 탄성파 탐사 기법을 연구하기에 매우 좋은 조건이며, 이 연구를 통한 조간대 퇴적체의 발달 형태, 발달과정 및 퇴적모델의 규명은 향 후 오일샌드 탐사 및 생산 분야에 반드시 필요함.

□ 해안 및 연안개발에 있어서 퇴적층 아래에 있는 기반암의 깊이와 공간적인 분포 파악은 매우 중요함. 현재까지는 해안 및 연안지역에서 기반암의 깊이와 이 깊이의 분포 파악을 위해서는 시간과 비용이 많이 소요되는 시추(drilling)방법이 이용되고 있음. 하지만 시추 방법은 시추 지점들 사이의 간격이 멀기 때문에 시추 지점 사이에 있는 지역에서 정확한 기반암의 깊이와 이 깊이의 분포 파악이 어려운 실정임. 따라서 현생 조간대 탄성파 탐사 기법 연구는 조간대 환경에서 기반암의 깊이와 이 깊이의 분포를 파악하는데 매우 효율적으로 사용될 수 있음.

□ 현생 조간대 탄성파 탐사 기법을 이용하여 파악된 현생 조간대 퇴적체의 장기적인 발달 양상은 퇴적체 발달에 영향을 미친 요인들의 상대적 기여도를 파악하게 해줌. 이러한 파악은 조간대 환경이 개발되면서 건설되는 인공 시설물에 따른 조간대 환경의 장기적인 변화 양상을 예측하는데 기초자료로 이용될 수 있음.

1.2. 목적

□ 현생 조간대환경에 적합한 탄성파탐사 기법 정립

□ 탄성파 자료와 시추퇴적물 자료를 이용하여 마지막 해수면 상승시기 동안 한반도 남·서해안에 분포하는 현생 조간대 퇴적체의 발달 양상

과 발달에 영향을 미치는 주요 요인(또는 인자) 규명

□ 한반도 남·서해안에 분포하는 현생 조간대 퇴적체의 퇴적모델 및 분류 정립

2. 국내·국외 연구개발 동향 및 분석

2.1. 관련연구/기술의 국내·국외 동향

국외 동향

□ 여러 종류의 육상 탄성파탐사 기법 중 GPR(Ground Penetrating Radar) 탐사 기법을 이용하여 현생 해빈(beach) 상부와 해안 사구에서 퇴적체 내부의 지질 특성을 규명하는 연구가 매우 활발하게 이루어지고 있음

□ GPR 탐사 기법을 현생 조간대 환경에 시도하였지만 현생 조간대 퇴적체내에 염분이 있는 공극수로 인해 현생 조간대에서 탄성파탐사 기법으로 이용하기 부적절한 상황

□ 주요 대형 외국석유회사와 외국 대학들은 오일샌드 탐사 및 생산에 필수적인 조간대 퇴적층의 퇴적모델을 정립하기 위하여 현생 조간대 환경에 효율적인 육상 탄성파탐사 기법을 파악, 테스트하고 발전시키는 초기 단계임

□ 일본 PARI (Port and Airport Research Institute)는 현생 조간대 퇴적체의 효율적인 관리, 보존 및 개발을 위해 일본 문부과학성의 대형 프로젝트를 통해 육상 탄성파 탐사 기법 중 하나인 MASW (multichannel analysis of surface waves) 기법을 도입하여 조간대 환경에 맞게 발전시키고 있음. 이 기법을 이용해 조간대 표층에서 5-7 m까지의 조간대 지층의 퇴적물 종류 및 분포에 관한 초기연구 결과를 2008년 Marine Geology에 발표함

국내 동향

□ 국내에서는 해수유입이 매우 적은 현생 사질 조간대 상부환경 및 해안사구지역에서 GPR 탐사 기법을 이용한 퇴적체에 관한 연구가 수행된 적이 있으나 해수 유입이 주기적으로 이루어지는 조간대 하부

및 중부지역에서 육상 탄성파 탐사 기법을 이용한 조간대 퇴적체에 관한 연구는 매우 미비한 실정임

□ 최근 전북대, 충북대 및 배재대 연구팀이 지자기를 이용하는 MT 탐사 방법을 이용하여 곰소만 조간대에서 기반암의 분포를 대략적으로 파악하는데 성공하였지만, 자료의 해상도가 매우 떨어져서 조간대 퇴적체의 특성을 규명하는데 실패함

□ 표층퇴적물, 현재 지형 및 길이가 짧은 캔코어 퇴적물을 이용하여 조간대의 표층에 관한 연구는 많이 이루어졌지만 조간대 퇴적체의 지층내부 특성 파악과 이를 통한 다양한 조간대 퇴적체의 분류에 관한 연구는 매우 미비함

2.2. 관련기술의 시장규모 및 적용가능 분야

가. 관련기술의 시장규모

□ 직접적인 해당사항은 없지만 연안관련 국내 컨설팅 회사와 석유관련 회사에 매우 유용하게 쓰일 수 있음

나. 관련기술의 적용가능 분야

기술분류	적용 가능 분야
해양과학기술	○ 영토(연안) 관리 관련 ○ 연안 해양환경 보존 및 개발 관련 ○ 해양환경 변화 연구 관련

2.3. 국내 연구개발 현황 및 능력분석

□ 현재까지 현생 조간대 환경에 적합한 탄성파탐사 기법에 관한 연구가 매우 미비함

□ 조간대에서 획득한 탄성파 자료를 전산처리한 경험이 미비함

□ 기존에 한반도 남·서해안에 분포하는 현생 조간대의 표층에서 획득된 많은 연구결과를 탄성파 자료와 결합하여 조간대 퇴적체 발달양상과 발달요인을 규명하는데 이용할 수 있음

2.4. 선진국 수준과의 비교

□ 해양선진국인 미국, 일본, 영국 등에서 현생 조간대 환경에 적합한 탄성파탐사 기법에 관한 연구를 체계적으로 하지 않았을 정도로 매우 초기 단계임

□ 해양선진국인 미국, 일본, 영국 등에서도 현생 조간대 탄성파탐사 자료를 이용하여 연안 해양환경 변화, 연안 보존 및 개발에 관한 연구에 활용된 적이 없음

3. 연구개발 목표

3.1. 최종 목표

□ 현생 사질, 니질 및 혼합질(니·사질) 조간대환경에 적합한 탄성파탐사 기법 정립

□ 탄성파 자료와 시추퇴적물 자료를 이용하여 마지막 해수면 상승시기 동안 한반도 남·서해안에 분포하는 현생 조간대 퇴적체의 발달 양상과 발달에 영향을 미치는 주요 요인(또는 인자) 규명

□ 한반도 남·서해안에 분포하는 현생 조간대 퇴적체의 퇴적모델 및 분류 정립

3.2. 단계별 연구목표

□ 1단계(2010년 ~2012년)

- 현생 사질 조간대환경에 적합한 탄성파탐사 기법 정립
- 한반도 남·서해안에 분포하는 현생 사질 조간대 퇴적체의 발달 양상 및 발달에 영향을 미치는 주요 인자 규명
- 한반도 남·서해안에 분포하는 현생 사질 조간대 퇴적체의 퇴적모델 정립

□ 2단계(2013년 ~2015년)

- 현생 니질/혼합질 조간대환경에 적합한 탄성파탐사 장비개발 및 기법 정립
- 한반도 남·서해안에 분포하는 현생 니질 및 혼합질 조간대 퇴적체

의 발달 양상 및 발달에 영향을 미치는 주요 인자 규명
- 한반도 남·서해안에 분포하는 현생 니질 조간대 퇴적체의 퇴적모델 정립

□ 3단계(2016년 ~2018년)
- 1~2 단계에서 정립된 퇴적모델과 발달에 영향을 미치는 주요 인자들을 종합하여 한반도 남·서해안에 분포하는 현생 조간대환경 및 퇴적체의 분류체계 정립

4. 연구내용 및 범위

4.1. 단계별 연구내용 및 범위

단 계	연구 내용 및 범위
1단계 (2010년~2012년)	▶ 현생 사질 조간대 연구지역 2~3 곳 선정 ▶ 현생 사질 조간대환경에 적합한 탄성파탐사 음원 및 수신장치 개발 ▶ 현생 사질 조간대환경에서 획득된 탄성파자료 처리기법 개발 ▶ 시추퇴적물을 이용하여 퇴적물 특성의 3차원 변화 파악 ▶ 현생 사질 조간대 퇴적체의 발달 양상 및 발달요인 규명 ▶ 현생 사질 조간대 퇴적체의 퇴적 모델 정립
2단계 (2013년~2015년)	▶ 현생 니질 및 혼합질(니·사질) 조간대 연구지역 2~3 곳 선정 ▶ 현생 니질 및 혼합질 조간대환경에 적합한 탄성파탐사 음원 및 수신장치 개발 ▶ 현생 니질 및 혼합질 조간대환경에서 획득된 탄성파자료 처리기법 개발 ▶ 시추퇴적물을 이용하여 퇴적물 특성의 3차원 변화 파악 ▶ 현생 니질 및 혼합질 조간대 퇴적체의 발달 양상 및 발달요인 규명 ▶ 현생 니질 및 혼합질 조간대 퇴적체의 퇴적 모델 정립
3단계 (2016년~2018년)	▶ 현생, 사질, 니질 및 혼합질 조간대 퇴적체의 퇴적 모델과 발달 요인들을 종합 ▶ 한반도 남·서해안에 분포하는 현생 조간대 환경 및 퇴적체의 분류

4.2. 연구대상의 개발 가능성

□ 현생 조간대환경에 적합한 탄성파탐사 기법 정립

- 최근 활발하게 개발된 첨단 육상 탄성파탐사 장비를 변형하여 조간대 환경에 적합한 탄성파탐사 장비를 개발할 가능성이 높음
- 연안지역과 육상에서 획득된 탄성파탐사 자료처리의 경험이 풍부하여 조간대 탄성파탐사 자료처리 기법을 정립하는데 어려움이 미비함

□ 한반도 남·서해안 현생 사질, 니질 및 혼합질 조간대 퇴적체의 퇴적모델 및 발달 요인 규명

- 최근 갯벌 환경의 보존에 관련되어 많은 해양학적, 지질학적 연구가 수행되어 다양한 종류의 자료와 연구 결과가 도출되었음. 이러한 자료와 연구 결과는 본 연구에 기초자료를 제공하여 한반도 남·서해안 현생 사질, 니질 및 혼합질 조간대 퇴적체의 퇴적모델 및 발달 요인을 규명하는데 가능성이 매우 높음

□ 한반도 남·서해안 현생 조간대 환경 및 퇴적체 분류 정립

- 조간대 환경에서 다학제간의 공동연구가 최근 활발하게 이루어지고 있음. 이러한 연구에서 도출된 퇴적역학적, 지화학적, 생태학적 요인들과 본 연구의 결과를 같이 종합하면 한반도 남·서해안 현생 조간대 환경 및 퇴적체를 합리적으로 분류하는데 가능성이 높음

4.3. 기술개발 및 점유 가능성

- 해당 사항 없음

5. 연구개발 추진전략 및 체계

5.1. 기본방안

□ 기존에 지질학적 연구가 활발하게 이루어진 조간대 지역 중 본 연구에 적합한 연구 지역 선정함

□ 육상 탄성파 탐사에서 음원으로 주로 해머, 자동 진동장치, 화약총 및 전자음파 등이 있는데 이 음원들 중에서 현생 조간대 환경에 적합한 음원을 파악하고 변형함

□ 육상에 탄성파 탐사에서 음파 탐지(수신) 장비로 지오폰(Geo-phone)

시스템이 주로 이용되는데 이 시스템을 변형하여 현생 니질 및 사질 조간대환경에 적합하게 수신 장치를 개발함

□ 처리된 탄성파 단면에 나타나는 음파 특성 및 형태와 시추 암상 자료를 비교하여 탄성파 자료의 해상도 및 효율성 파악하여 현생 조간대 탄성파탐사 자료처리 기법을 정립함

□ 탄성파 자료, 시추 암상자료, 해양 작용 자료를 합쳐서 현생 사질 조간대 지층의 퇴적단위 구분, 각 퇴적단위의 퇴적/침식작용, 발달 양상 및 발달 요인을 규명하고 마지막 해수면 상승시기동안의 한반도 남·서해안 현생 조간대 퇴적체의 퇴적 모델을 수립

□ 퇴적역학, 생태학 및 지화학 연구 분야의 결과를 종합·비교하고 이들 분야와의 공동 연구를 통해 한반도 남·서해안 현생 조간대 환경 및 퇴적체를 다학제간에서 활용할 수 있는 분류체계를 정립

5.2. 추진전략

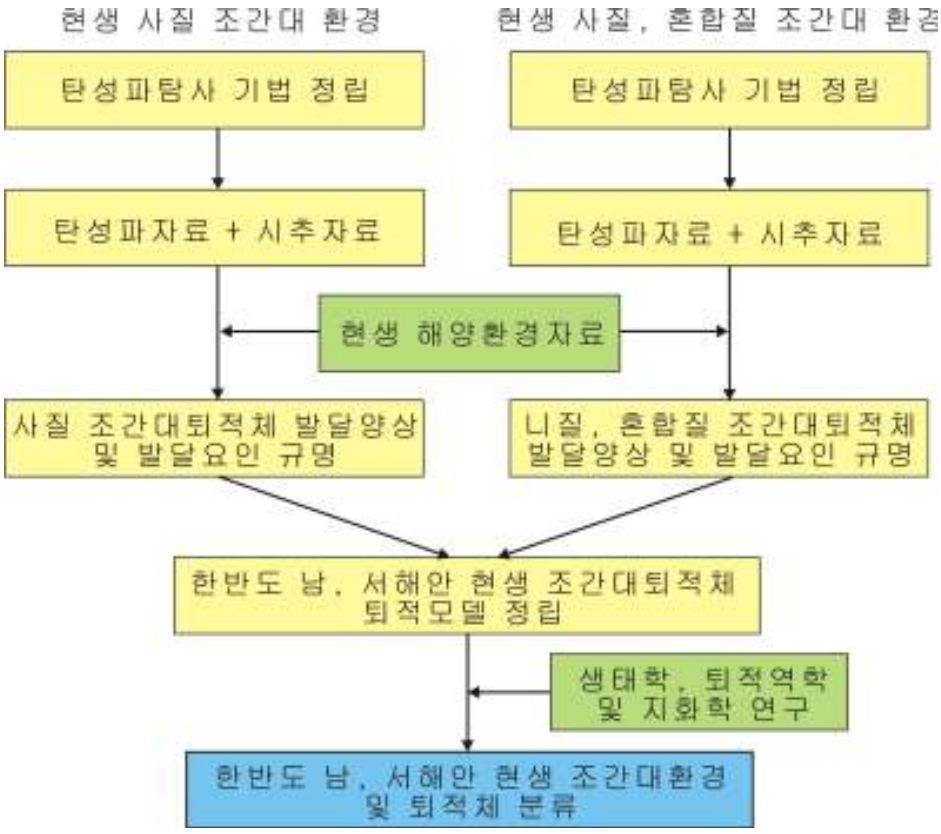

5.3. 연구개발 추진일정

분류	핵심기술 연구내용	1단계			2단계			3단계			비고
		10	11	12	13	14	15	16	17	18	
	- 현생 사질 조간대환경에 적합한 탄성파탐사 기법 정립 - 현생 사질 조간대 퇴적체의 발달 양상 및 발달요인 규명 - 현생 사질 조간대 퇴적체의 퇴적모델 정립	■	■	■							
	- 현생 니질·혼합질 조간대환경에 적합한 탄성파탐사 장비개발 및 기법 정립 - 현생 니질·혼합질 조간대 퇴적체의 발달 양상 및 발달요인 규명 - 현생 니질 조간대 퇴적체의 퇴적모델 정립				■	■	■				
	- 한반도 남·서해안 현생 조간대 환경 및 퇴적체의 분류							■	■	■	

6. 기대성과 및 활용방안

6.1. 기대성과

□ 현생 조간대 환경에 적합하고 효율적인 탄성파 탐사 기법 정립과 탐사 장비 개발

□ 한반도 남·서해안 현생 조간대의 분류체계는 다학제간에서 이용할 수 있음

□ 효과적인 조간대 퇴적체 또는 조간대 환경의 관리 및 보존을 위한 중요 기초자료 제공

□ 현생 조간대 퇴적체의 퇴적 모델 수립은 오일샌드의 근원암과 저류암을 파악하는 탐사 및 생산 분야에 응용

□ 현생 조간대 환경에서 인공시설물 건설에 필수적인 기반암 깊이 및 깊이 분포 파악을 위한 효율적인 탐사기법 제공

□ 유류 오염에 따른 조간대 환경 및 퇴적체에 대한 방제 및 복원에 필수적인 자료 제공

6.2. 활용방안

□ 조간대 퇴적층에서 주로 생산되는 오일샌드관련 지식경제부 및 한국석유공사의 국가 대형연구 프로젝트에 참여할 수 있는 기반으로 활용

□ 한반도 서해안 및 남해안에 분포하는 다양한 현생 조간대 환경(퇴적체)의 분류 및 분류도 작성은 조간대 환경의 효율적인 관리 및 개발을 위해 필수적이기 때문에 기존에 수행된 해양환경도 및 해양자원도와 같은 개념으로 정부로부터 장기적인 국가해안 분류도 연구 프로젝트의 개발에 활용

□ 조간대 퇴적체의 내부 특성은 퇴적층에 유입된 유출 유류의 이동과 집적 양상을 결정하는 중요한 요인이기 때문에 향 후 해안퇴적물에서의 유출 유류의 의한 오염의 방제와 복원에 관한 연구 프로젝트 개발에 활용

7. 결론

□ 한반도 서해안 및 남해안에 광범위하게 분포하는 다양한 현생 조간대 환경의 효율적인 관리 및 개발을 위해 본 연구를 통해 도출되는 이들 현생 조간대환경 및 퇴적체의 분류체계가 반드시 필요함

□ 한반도 남·서해안 현생 조간대 퇴적체의 특성과 발달 양상은 해안오염에 따른 조간대 저서생태계의 방제 및 복원에 필수적임

□ 현생 니질, 혼합질 및 사질 조간대 퇴적체의 퇴적모델 수립은 조간대 퇴적층에서 주로 생산되는 오일샌드관련 지식기반에 중요한 기초자료로 이용될 수 있어 본 연구는 매우 중요함

8. 소요예산

□ 총 연구비 : 37.5억(9 년간) (단위 : 억원)

분 야	1단계			2단계			3단계			합 계
	'10	'11	'12	'13	'14	'15	'16	'17	'18	
본 연구	5	5	5	5	5	5	2.5	2.5	2.5	37.5

- 첨부: SCI 논문 -

Marine Geology xxx (2009) xxx–xxx

Contents lists available at ScienceDirect

Marine Geology

journal homepage: www.elsevier.com/locate/margeo

Depositional development of an isolated mound and adjacent area in the southern Yellow Sea during the last postglacial sea-level rise

S.H. Lee [a,*], Y.J. Shinn [b,1], K.E. Lee [c], H.S. Yoo [a]

[a] Marine Geology and Geophysics Laboratory, Korea Ocean Research and Development Institute, Ansan P. O. Box 29, Seoul 425-600, South Korea
[b] School of Earth and Environmental Sciences, Seoul National University, Seoul 151-747, South Korea
[c] Division of Marine Environment and Bioscience, Korea Maritime University, Busan 606-791, South Korea

ARTICLE INFO

Article history:
Received 30 October 2008
Received in revised form 15 June 2009
Accepted 18 June 2009
Available online xxxx

Communicated by J.T. Wells

Keywords:
transgressive deposits
highstand deposits
sea-level rise
Holocene
Yellow Sea

ABSTRACT

A detailed analysis of the Chirp (2–7 kHz) profiles, core sediments and ^{14}C ages from an isolated mound and adjacent area in the southern Yellow Sea off the Jiangsu coastal area reveals a highly complex development of transgressive and highstand deposits during the last postglacial sea-level rise. In water depths of 50–60 m, the terrace consists of thin transgressive sediments directly above transgressive surface. The isolated mound (40.7 km long and 29.6 km wide) occurs above 40–50 m in water depth, and is detached from the Jiangsu and East China Sea tidal sand ridges. It comprises the SSE-ward prograding sandy unit (PU) and the overlying muddy flank unit (FU) at the outer margin. The terrace with thin transgressive sediments was most likely formed when sea level rose rapidly from −58 to −45 m around about 11.6 ka. As rate of sea-level rise was attenuated from −45 to −36 m between ca. 11.6 and 9.6 ka, the nearly flat lower boundary of the PU was produced at water depths of 37–42 m by a ravinement process. Subsequent rapid sea-level rise from −36 to −16 m between ca. 9.6 and 9.1 ka created accommodation for deposition of the PU. Sea-level rise stagnated from −16 to −10 m between ca. 9.1 and 7.5 ka during which the Huanghe River apparently shifted south of the Shandong Peninsula and discharged directly into the western Yellow Sea. The combination of slow sea-level rise and sediment supply from the early Holocene Huanghe delta by the southward-flowing coastal currents most likely favoured the formation of the SSE-ward prograding transgressive sandy PU. The highstand muddy FU overlying the PU was accumulated after ca. 7.5 when sea level approached its present position and the Huanghe River shifted back to the north. Development of transgressive and highstand deposits in the study area during the last postglacial sea-level rise was highly variable in time and space in response to changes in rate of sea-level rise together with variations in sediment supply caused by the shifting of the Huanghe River.

1. Introduction

The Yellow Sea is a low-gradient epicontinental sea that underwent complete subaerial exposure during the last glacial maximum (Fairbanks, 1989; Pirazzoli, 1991). As sea level rose, a variety of transgressive and highstand sedimentary bodies were formed in response to changes in rate of sea-level rise together with spatial–temporal variations in sediment supply, oceanic and tidal currents, and waves (Milliman et al., 1989; Alexander et al., 1991; Lee and Yoon, 1997; Park et al., 2000; Lee and Chu, 2001; Jin et al., 2002; Uehara and Saito, 2003; Chough et al., 2004; Liu et al., 2004, 2007; Shinn et al., 2007). Relatively high amplitude sea-level rise in the early to middle transgression strongly affected sedimentation to produce transgressive sand sheets/veneers and sediment ridges (Lee and Yoon, 1997; Jin and Chough, 2002; Chough et al., 2002; Liu et al., 2004; Shinn et al., 2007). As the rate of sea-level rise decreased, depositional processes were mostly influenced by sediment supply, topography and prevailing currents, forming transgressive to highstand Heuksan mud bank, Shandong mud wedge, central Yellow Sea mud and Jiangsu tidal sand ridges (Jin and Chough, 1998; Lee and Chu, 2001; Li et al., 2001; Chough et al., 2002; Liu et al., 2002, 2004, 2007; Yang and Liu, 2007). Depositional features, history and occurrences of these various transgressive and highstand deposits could provide invaluable information on high-resolution sequence stratigraphic development in a low-gradient, high-energy epicontinental shelf setting.

High-resolution depositional development of the Shandong mud wedge and Jiangsu tidal sand ridges in the western coastal area of the Yellow Sea has been well understood (Li et al., 2001; Liu et al., 2002, 2004, 2007; Yang and Liu, 2007). However, detailed development of the last postglacial transgressive and highstand sedimentary bodies in offshore area (ca. 30–65 m in water depth) between the central Yellow Sea (Yellow Sea Trough) and the western coastal area of the Yellow Sea (Jiangsu coastal area) has been poorly known, even though

* Corresponding author. Tel: +82 31 400 7659; fax: +82 31 400 6288.
E-mail address: sanglee@kordi.re.kr (S.H. Lee).
[1] Present address: Korea Institute of Geosciences and Mineral Resources, Yuseong, Daejeon 305-350, South Korea.

0025-3227/$ – see front matter © 2009 Elsevier B.V. All rights reserved.
doi:10.1016/j.margeo.2009.06.010

a few Chinese local studies documented roughly late Quaternary stratigraphy in this offshore area using widely spaced seismic profiles and cores (e.g., Yang, 1985; Shi et al., 1986). Because this offshore area is a linkage between the Yellow Sea Trough and Jiangsu coastal area, detailed depositional processes, geometry and history in this offshore area are crucial to fully understand high-resolution sequence stratigraphic development of the western Yellow Sea during the last postglacial sea-level rise. Recent close-spaced (ca. 2–3 km) high-resolution Chirp (2–7 kHz) surveys revealed an isolated mound surrounded by nearly flat, featureless sand-veneer deposits in the southern part of this offshore area (Shinn et al., 2007). The isolated mound is not directly connected to two well-known (Jinagsu and East China Sea) tidal sand ridges which occur relatively close to the study area (Fig. 1A). This paper details high-resolution acoustic characters, core-sediment lithology and ^{14}C ages of the isolated mound and adjacent area in order to propose their depositional development in terms of rate of sea-level rise, sediment supply and oceanographic regime.

2. Regional settings

2.1. Physiography

The Yellow Sea is a shallow, low-gradient epicontinental sea bounded by the landmass of Korea and China. The Yellow Sea is less than 100 m in water depth, with an average water depth of about 55 m. The seafloor deepens toward a NW–SE-trending depression (Yellow Sea Trough), defined by the 80-m isobath (Fig. 1A). Toward the Chinese coast, the seafloor is rather flat within the water depth of 50 m, and is generally interrupted by slopes between 50 and 60 m in water depth. The study area occurs at water depths of ca. 35–60 m between the Yellow Sea Trough and the Jiangsu coastal area (Fig. 1A). In the inner to middle shelf areas along the west coast of Korea, the seafloor is characterized by ridge-and-swale morphology (Chough et al., 2002).

2.2. Oceanographic setting

The Yellow Sea is dominated by semi-diurnal tides with a tidal range exceeding 4 m in many coastal areas and less than 2 m in the central part (Choi, 1980). Numerical model of tidal current ellipses shows a rectilinear pattern in the west coast of Korea and Changjiang River mouth and a distinctive radial pattern near the Jiangsu coast (Fig. 2A; Lee and Jung, 1999). Tidal currents generally exceed 100 cm/s in the nearshore area, and decrease to the central part (Larsen et al., 1985; Teague et al., 1998). Two-dimensional paleotidal model displays the region of intense tidal bottom stress migrated shoreward from Jeju Island toward the southwest coast of Korea and along the retreat path of the paleo-Changjiang estuary as sea level rose (Uehara and Saito, 2003).

General circulation in the Yellow Sea shows a counter-clockwise gyre (Fig. 2B). The Yellow Sea warm current (YSWC), a branch of Kuroshio Current, flows northward into the southeastern Yellow Sea (Fig. 2B) and carries warm, saline water into the Yellow Sea (Guan, 1994). The YSWC intrudes into the northern Yellow Sea during winter

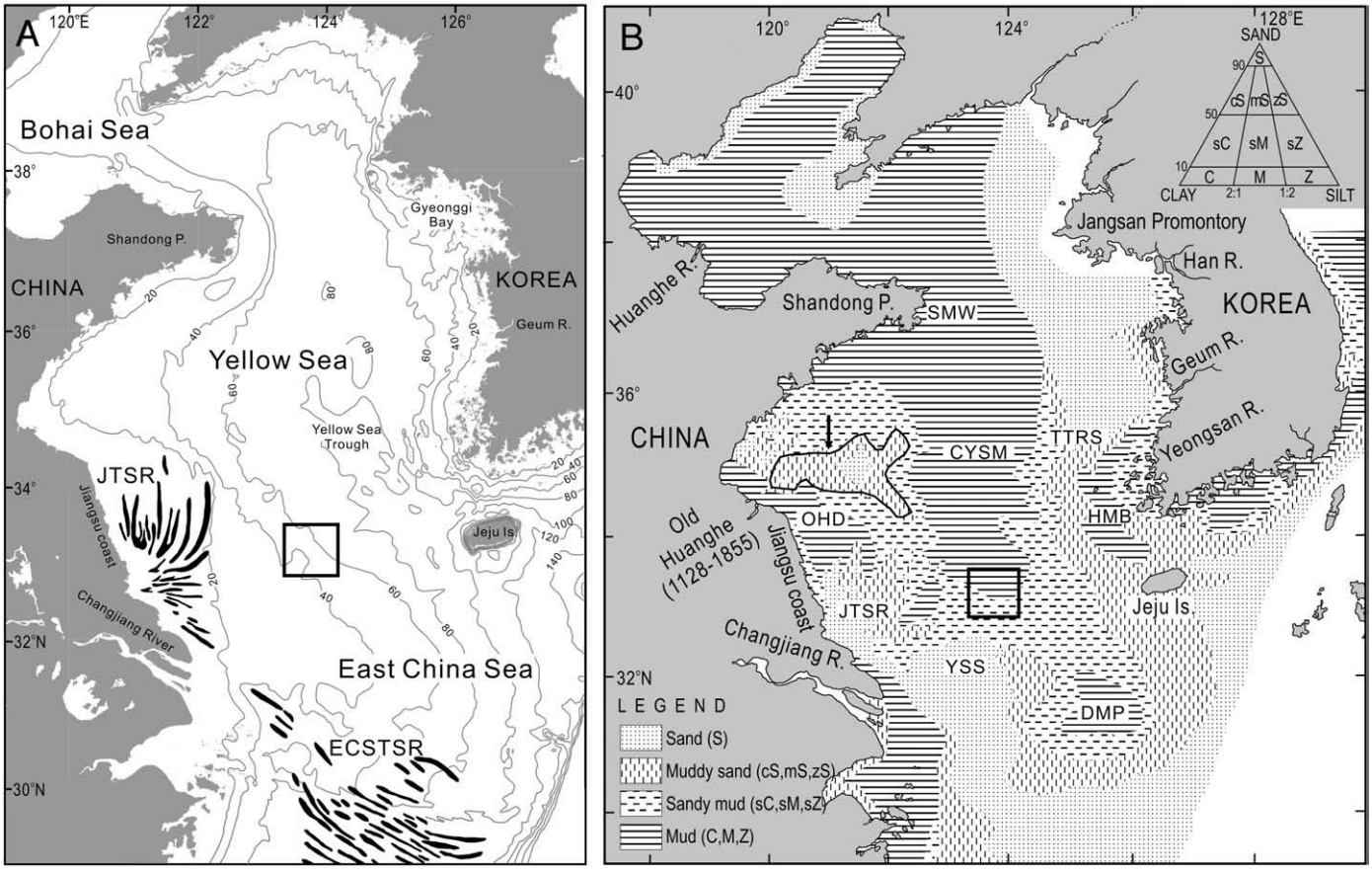

Fig. 1. (A) A map showing bathymetry of the Yellow Sea and adjacent seas together with distribution of tidal sand ridge systems (black areas). JTSR = Jiangsu tidal sand ridges; ECSTSR = East China Sea tidal sand ridges. Location of the JTSR and ECSTSR from Liu et al. (1989), Berné et al. (2002) and Chen et al. (2003). Contours in meters. (B) Distribution of surface sediments in the Yellow Sea and adjacent seas (modified from Lee and Chough, 1989). OHD = old Huanghe delta formed between 1128 and 1855 AD; CYSM = central Yellow Sea mud; DMP = distal mud patch; HMB = Heuksan mud belt; JTSR = Jiangsu tidal sand ridge; SMW = Shandong mud wedge; TTRS = transgressive tidal ridge and swale; YSS = Yangtze sand shoal. A bold box in (A) and (B) indicates the study area. An arrowed area in (B) apparently represents the erosional remnants of the early Holocene Huanghe deltaic sediments (Milliman et al., 1987, 1989; Alexander et al., 1991).

Please cite this article as: Lee, S.H., et al., Depositional development of an isolated mound and adjacent area in the southern Yellow Sea during the last postglacial sea-level rise, Mar. Geol. (2009), doi:10.1016/j.margeo.2009.06.010

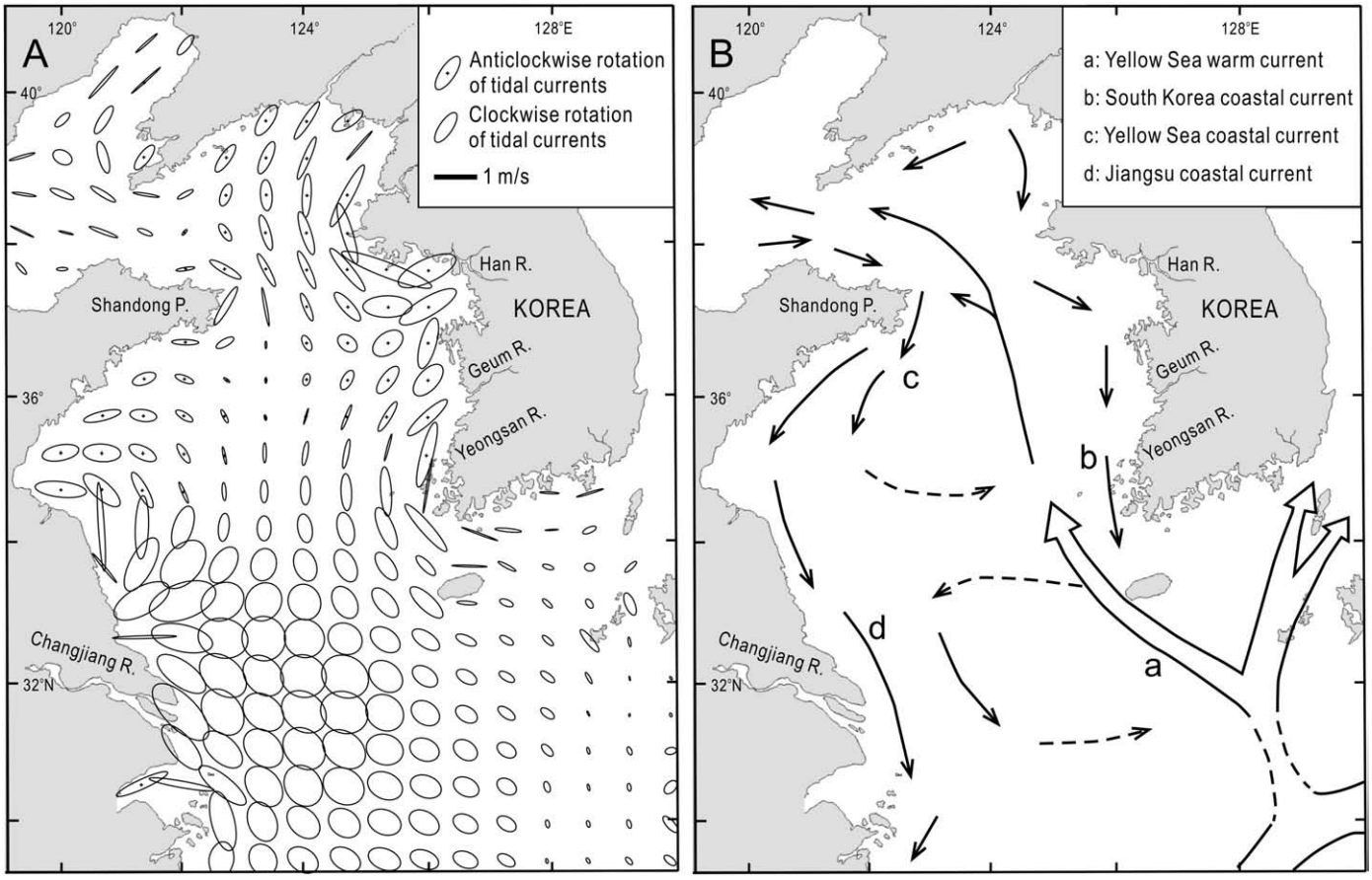

Fig. 2. (A) M_2 tidal model of the Yellow Sea and adjacent seas (modified from Lee and Jung, 1999). (B) Regional circulation pattern in the Yellow Sea and adjacent seas for winter (modified from Guan, 1994).

when the shelf-water column is nearly homogenous. The Yellow Sea cold water occurs in the central Yellow Sea during the warm half of the year (April–November), forming smaller, semi-permanent circulation in the central and southern Yellow Sea (Su and Weng, 1994). Along the Chinese coast, the Yellow Sea and Jiangsu coastal currents flow southward during both summer and winter (Fig. 2B; Beardsley et al., 1983). East Asian monsoonal winds cause local currents and circulation, facing toward the northwest in summer and the southwest in winter (Hseuh, 1984; Wells and Huh, 1984).

2.3. Geologic setting

The Yellow Sea was subaerially exposed during the last glacial period when sea level was lowered by about 120 m below the present level (Fairbanks, 1989; Pirazzoli, 1991). After the last glacial maximum (LGM), the sea level rose with various rates (Bloom and Park, 1985; Pirazzoli, 1991; Chough et al., 2000). In the Yellow Sea, the post-LGM sea-level curve was stepwise: long-term slow rises interrupted by several short, rapid rises (Liu et al., 2004). In the central part of the Yellow Sea, marine transgression began at about 11–12 ka (Wang et al., 1985; Kim and Kennett, 1998). The sea level reached its present position at ca. 7–7.5 ka (Chen and Stanley, 1998; Kim et al., 1999).

The Yellow Sea receives a large amount of sediments from the landmass of China and Korea through a number of rivers (Milliman et al., 1985; Chough et al., 2000). The Huanghe River discharges about 1.08×10^9 t/yr of sediments (Milliman and Meade, 1983), and it is a major source for the Holocene muddy sediments (i.e., the Shandong mud wedge and central Yellow Sea mud) in the Yellow Sea (Liu et al., 2004, 2007; Shinn et al., 2007). From 1128 to 1855 AD, the Huanghe River flowed south of the Shandong Peninsula, forming subaqueous delta lobes (old Huanghe delta) along the Jiangsu coast (Fig. 1B; Milliman et al., 1987, 1989). Before the 1128 AD shifting, the river probably shifted to the south in response to extremely heavy flood around about 9 ka and discharged directly into the western Yellow Sea for the next ca. 1.5–2 ky (Milliman et al., 1987; Yang et al., 2000; Liu et al., 2002, 2004). The Changjiang River discharges ca. 5×10^8 t/yr (Milliman and Meade, 1983). Sediments derived from the Changjiang River are mostly confined to the south and seasonally transported offshore by plume event (Lee and Chough, 1989; Liu et al., 2006). Compared to the Chinese rivers, the Korean rivers discharge relatively small amounts of sediments into the eastern Yellow Sea (Chough et al., 2000).

In the Yellow Sea, various transgressive deposits occur above the subaerially exposed sediments as sea level rose after the LGM. Transgressive deposits in the central Yellow Sea are comprised of estuarine channel fills, sand veneers and mud blanket (Shinn et al., 2007). In the west coast of Korea, the deposits consist mostly of estuarine/tidal sediments and erosional ridges with the overlying sand sheets and veneers (Lee and Yoon, 1997; Jin and Chough, 2002). A thick subaqueous mud clinoform (Shandong mud wedge) occurs in the eastern tip of the Shandong Peninsula (SMW in Fig. 1B), which began to accumulate at about 11 ka (Liu et al., 2004, 2007). After the sea level approached its present position at about 7–7.5 ka, different hydrodynamic conditions affected shelf sedimentation, forming highstand and regressive deposits in the Yellow Sea. Muds derived from the Huanghe River accumulated in the central part of the Yellow Sea (CYSM in Fig. 1B). Large-scale radial sand ridges occur north of the Changjiang River mouth off the Jiangsu coast (JTSR in Fig. 1A), which were formed by tidal currents during the regressive phase of seal level (Li et al., 2001).

Please cite this article as: Lee, S.H., et al., Depositional development of an isolated mound and adjacent area in the southern Yellow Sea during the last postglacial sea-level rise, Mar. Geol. (2009), doi:10.1016/j.margeo.2009.06.010

3. Materials and methods

High-resolution seismic profiles were acquired using a Chirp profiling system (Datasonics CAP-6000 W) by the National Oceanographic Research Institute of Korea. The Chirp profiling system is a tuned-frequency profiler that emits a computer-generated, frequency-modulated swept pulse with a frequency band of 2–7 kHz as a source signal. Returning signals were processed using a match-filtered correlation method to collect the same frequency band, providing higher-resolution images than those of the 3.5-kHz system (LeBlanc et al., 1992). Navigation was controlled using a Differential Global Positioning System (Trimble 4000 RS/DS) whose accuracy is within a few meters.

In order to provide ground truth of high-resolution acoustic characters, seven (172–359 cm long) piston cores were obtained by the Korea Ocean Research and Development Institute. All cores were split lengthwise and X-radiographs of 1-cm thick slab were taken to observe sedimentary structures. Grain size was analyzed using standard sieves and a Micrometrics Sedigraph 5100 for sand and mud fractions, respectively.

The ages of core sediments were determined by radiocarbon dating. Ten AMS ^{14}C dating of monospecific benthic foraminifera (*Ammonia beccarii*) and intact shells from bioturbated muds were performed at Rafter Laboratory, Geological and Nuclear Sciences in New Zealand (Table 1). The ^{14}C ages were calibrated using the values in the Yellow Sea of Stuiver et al. (2005). Calendar ages were converted from radiocarbon ages using CALIB 5.0 (Stuiver et al., 2005).

In this study, the postglacial sea-level curve of Liu et al. (2004) is used in order to propose the depositional development of sedimentary bodies in terms of sea-level changes. Liu et al. (2004) synthesized more than 100 data obtained from swamp (peat), intertidal–subtidal and shallow marine environments in the Yellow and East China seas for reconstruction of the post-LGM sea-level curve. Furthermore, they combined the data of Sunda (Hanebuth et al., 2000) and Bonaparte (Yokoyama et al., 2000) seas in order to check the trends of sea-level changes in the Yellow and East China seas.

4. Sedimentary features of the mound and adjacent area

4.1. Acoustic characters

The mound occurs as an isolated form above the water depths of 40–50 m (Fig. 3). It is about 40.7 km long, 29.6 km wide, and less than 15 m high. The mound is slightly elliptical in shape elongated to the N–S direction in plan view (Fig. 3). In longitudinal (N–S) cross section, the mound shows slightly asymmetrical shape, whereas it is nearly symmetrical in transverse (E–W) cross section (Fig. 4). Around the mound, the seafloor is generally characterized by nearly flat topography at water depths of ca. 40–50 m, changing northward and eastward to terrace-like morphology at water depths of 50–60 m (Fig. 4).

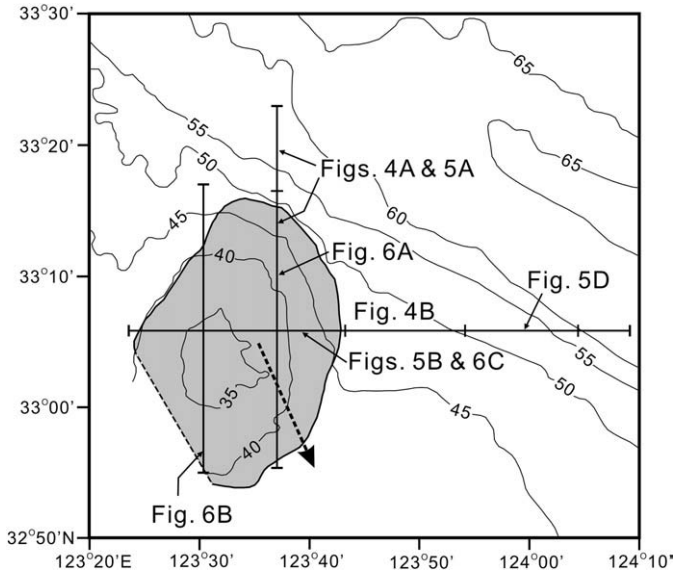

Fig. 3. Detailed bathymetry of the study area and distribution of the mound (gray area). A dotted arrow indicates the SSE-ward prograding direction of the prograding unit in the mound.

In the Chirp (2–7 kHz) profiles, the mound consists of prograding (PU) and flank (FU) units (Fig. 5). The PU is less than ca. 10 m thick. It is characterized by the southward prograding inclined internal reflectors in longitudinal (N–S) section (Figs. 5A and 6). On the other hand, the internal reflectors show slightly eastward-skewed, aggrading convex-up geometry in transverse (E–W) section (Figs. 5B and 6). This geometry of internal reflectors indicates that the PU prograded to the SSE. Internal reflectors in the PU downlap onto the lower bounding surface (Figs. 5A, B and 6). The lower bounding surface is nearly flat with slightly irregular relief, and occurs at about 37–42 m below the sea surface. Below the lower bounding surface, channel-fill deposits are preserved. The channel-fill deposits show partly horizontal to inclined internal reflectors which are eroded by the lower bounding surface of the PU (Fig. 5A, B). Inclined internal reflectors in the PU initially developed over the convex-up (i.e., mound-like) lower bounding surface in the northernmost part (Fig. 5A, C, open arrows). The internal reflectors in the PU are truncated by the lower boundary of the FU and the seafloor at the top (Figs. 5 and 6). The PU is overlain by the FU at the outer margin of mound (Figs. 5A, B and 6). The FU is less than about 6.5 m thick and thickens toward the outer margin. It consists of diffuse internal reflectors which onlap toward the center of mound upon the lower boundary (Figs. 5A, B and 6). The flat and terraced seafloor is characterized by sharp surface echo and highly prolonged subbottom echoes with a discontinuous, thin (less than 1–1.5 m thick) transparent layer in the uppermost part below the seafloor (Fig. 5A, D).

Table 1
^{14}C ages of benthic foraminifera and intact shells from bioturbated muds.

Core no.	Depth (cm)	Materials	Laboratory no.	AMS ^{14}C ages (yr BP)	Calendar age (cal yr BP)
2	299	Benthic foraminifera	NZA30134	3300 ± 35	3158 ± 39
2	319	Benthic foraminifera	NZA30135	3818 ± 35	3771 ± 40
2	328	Benthic foraminifera	NZA30136	4507 ± 35	4736 ± 44
3	88	Molluscan shell	NZA27140	1839 ± 30	1369 ± 25
3	105	Benthic foraminifera	NZA30253	2785 ± 20	2521 ± 54
4	26	Benthic foraminifera	NZA30256	3332 ± 20	3196 ± 35
4	35.5	Molluscan shell	NZA27145	6959 ± 30	7454 ± 23
5	77.5	Benthic foraminifera	NZA30255	3545 ± 20	3422 ± 27
5	121.5	Benthic foraminifera	NZA30258	4077 ± 20	4122 ± 30
6	123	Gastropod shell	NZA27142	2884 ± 25	2689 ± 20

4.2. Sedimentary facies

On the basis of grain size, color and hardness of sediments, and sedimentary structures on X-radiographs, core sediments are classified into eight sedimentary facies.

4.2.1. Massive sand (MS)

This facies is characterized by well sorted, massive medium sand with 90–96% in sand content (Figs. 7A and 8). It ranges from 2.31 to 2.46ϕ in mean grain size, and is 5–158 cm thick. The lower boundaries are generally sharp and erosive. This facies usually occurs at the uppermost part of the cores below the seafloor (Fig. 9).

Please cite this article as: Lee, S.H., et al., Depositional development of an isolated mound and adjacent area in the southern Yellow Sea during the last postglacial sea-level rise, Mar. Geol. (2009), doi:10.1016/j.margeo.2009.06.010

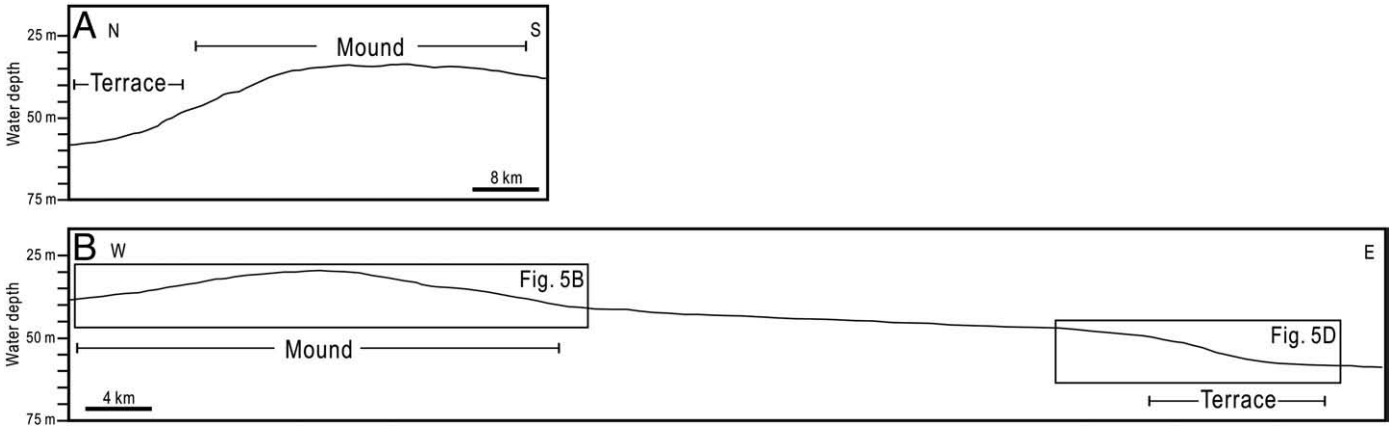

Fig. 4. Cross-sectional seafloor morphology of the mound and adjacent areas. Note a terrace-like morphology at water depths of ca. 50–60 m. For location of each profile, see Fig. 3.

4.2.2. Bioturbated muddy sand (BmS)

Facies BmS is represented by severely bioturbated, mottled, dark greenish muddy sand with 47–76% of sand (Figs. 7B, 8 and 10). It ranges from 3.94 to 5.04ϕ in mean grain size. Size distributions of sand generally display fine-sand mode (Fig. 8). In this facies, intact shells and shell fragments are nearly absent (Fig. 7B), and a very small amount of foraminifera are included. A few laminations are usually disturbed by bioturbation (Fig. 7B).

4.2.3. Gravelly mud (gM)

This facies is characterized by hard (semi-lithified), brownish mud clasts in muds (Fig. 7C). The clasts are 0.5–5 cm long, and partly clast-supported. Facies gM is 5–20 cm thick. The lower boundaries are sharp, erosive (Fig. 7C). This facies is generally underlain by hard, brownish sediment (facies HBS) (Figs. 7C and 9).

4.2.4. Laminated mud (LM)

Facies LM comprises horizontal to low-angle cross laminated, olive green mud with rare to slight bioturbation (Fig. 7E, F). Some bi-directional cross laminations are present. This facies ranges from 7.96 to 9.06ϕ in mean grain size with over 56% of clay (Fig. 8). It is less than 10 cm thick, and is usually associated with bioturbated mud (facies BM) (Fig. 9).

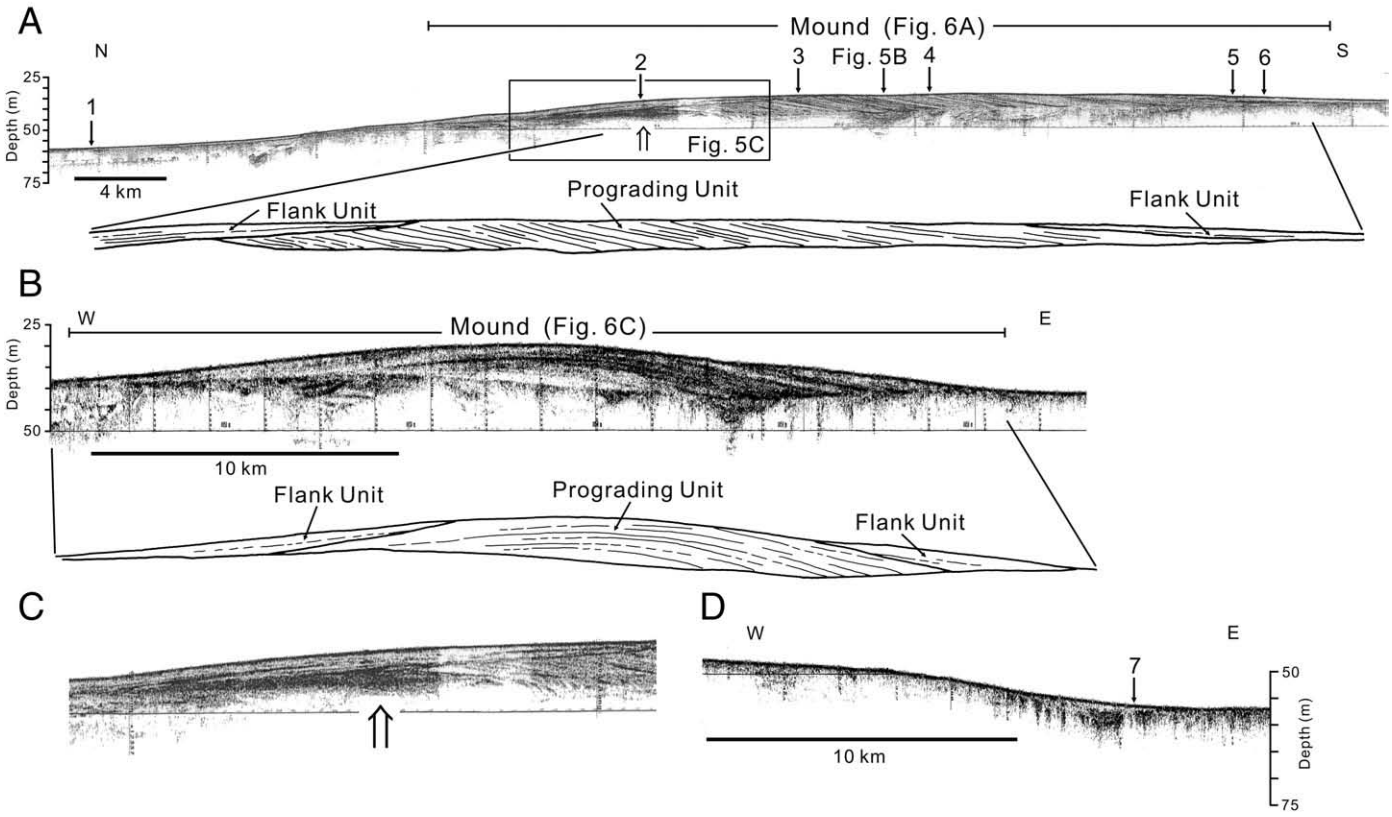

Fig. 5. (A), (B) and (C) Chirp (2–7 kHz) profiles and line drawings showing internal geometry of the mound in longitudinal (N–S) and transverse (E–W) sections. (D) A Chirp (2–7 kHz) profile exhibiting acoustic characters of flat and terraced seafloor. Arrows with numbers in (A) and (D) indicate location of cores. For location of each profile, see Figs. 3 and 4.

Please cite this article as: Lee, S.H., et al., Depositional development of an isolated mound and adjacent area in the southern Yellow Sea during the last postglacial sea-level rise, Mar. Geol. (2009), doi:10.1016/j.margeo.2009.06.010

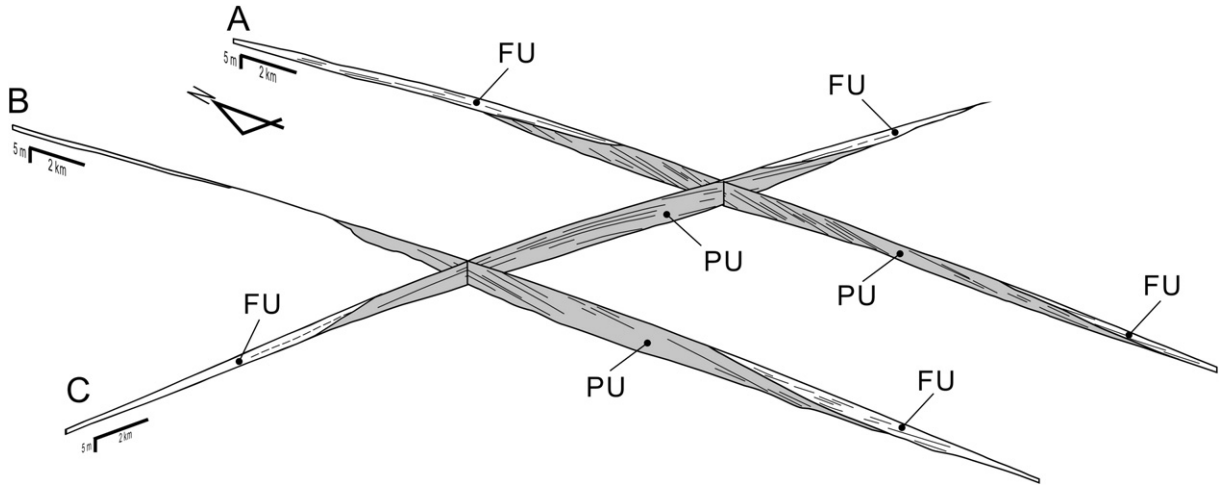

Fig. 6. A fence diagram showing external and internal geometry of the prograding (PU) and flank (FU) units in the mound. For location of profiles, see Figs. 3 and 5.

4.2.5. Homogeneous mud (HM)

This facies is represented by poorly sorted, light olive gray mud with over 50% of clay (Figs. 7E and 8). It ranges from 7.97 to 8.37ϕ in mean grain size. This facies is less than 10 cm thick, and is generally underlain by gravelly mud (facies gM) and massive sand (facies MS) (Fig. 9).

4.2.6. Bioturbated mud (BM) and sandy mud (BsM)

Facies BM and BsM comprise severely bioturbated, mottle, olive green mud and sandy mud, respectively (Fig. 7F–H). A few laminations are severely disturbed by bioturbation. Facies BsM ranges from 6.09 to 7.49ϕ in mean grain size with less than 30% of sand (Fig. 8). Facies BM displays 8.26–9.09ϕ in mean grain size with over 43% of clay (Figs. 8 and 10). These facies include a few intact shells (Fig. 7G) and relatively abundant foraminifera. Facies BM is generally associated with laminated mud (facies LM) (Fig. 9).

4.2.7. Hard brownish sediment (HBS)

This facies comprises hard (semi-lithified), brownish sandy to muddy sediments (Fig. 7C, D). It commonly includes cracks and oxidized grains (Fig. 7D). This facies is generally overlain by gravelly mud (facies gM) with a sharp, erosive boundary (Figs. 7C and 9).

4.3. Lithological characters and ^{14}C ages

In the mound, core sediments (core 4) from the PU consist mostly of bioturbated sand (facies BmS) with the uppermost (ca. 38 cm thick) bioturbated mud (facies BM) (Fig. 9). On the other hand, sediments

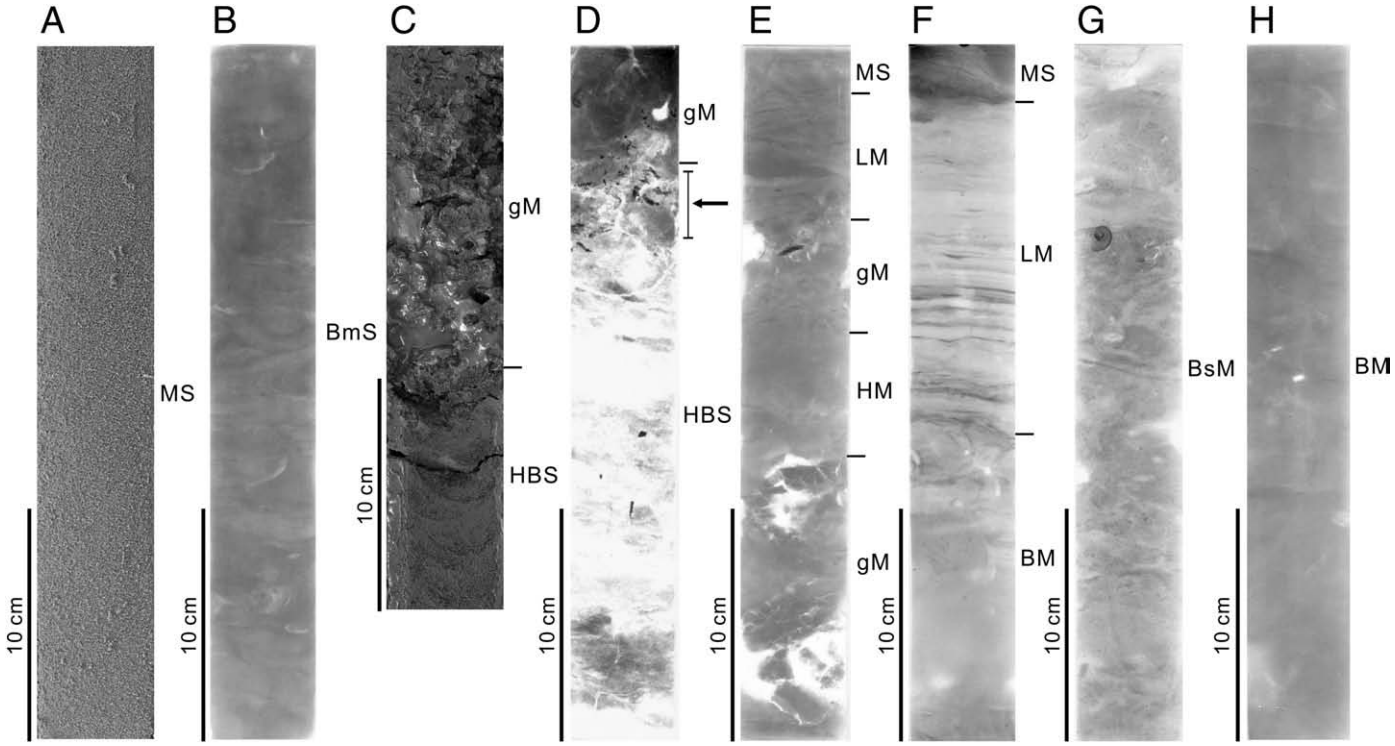

Fig. 7. Core photographs (A and C) and X-radiographs (B, D, E., F, G and H) of core sediments. Note common cracks and oxidized grains in facies HBS (black arrow in D). MS = massive sand; BmS = bioturbated muddy sand; gM = gravelly mud; LM = laminated mud; HM = homogeneous mud; BsM = bioturbated sandy mud; BM = bioturbated mud; HBS = hard brownish sediment.

Please cite this article as: Lee, S.H., et al., Depositional development of an isolated mound and adjacent area in the southern Yellow Sea during the last postglacial sea-level rise, Mar. Geol. (2009), doi:10.1016/j.margeo.2009.06.010

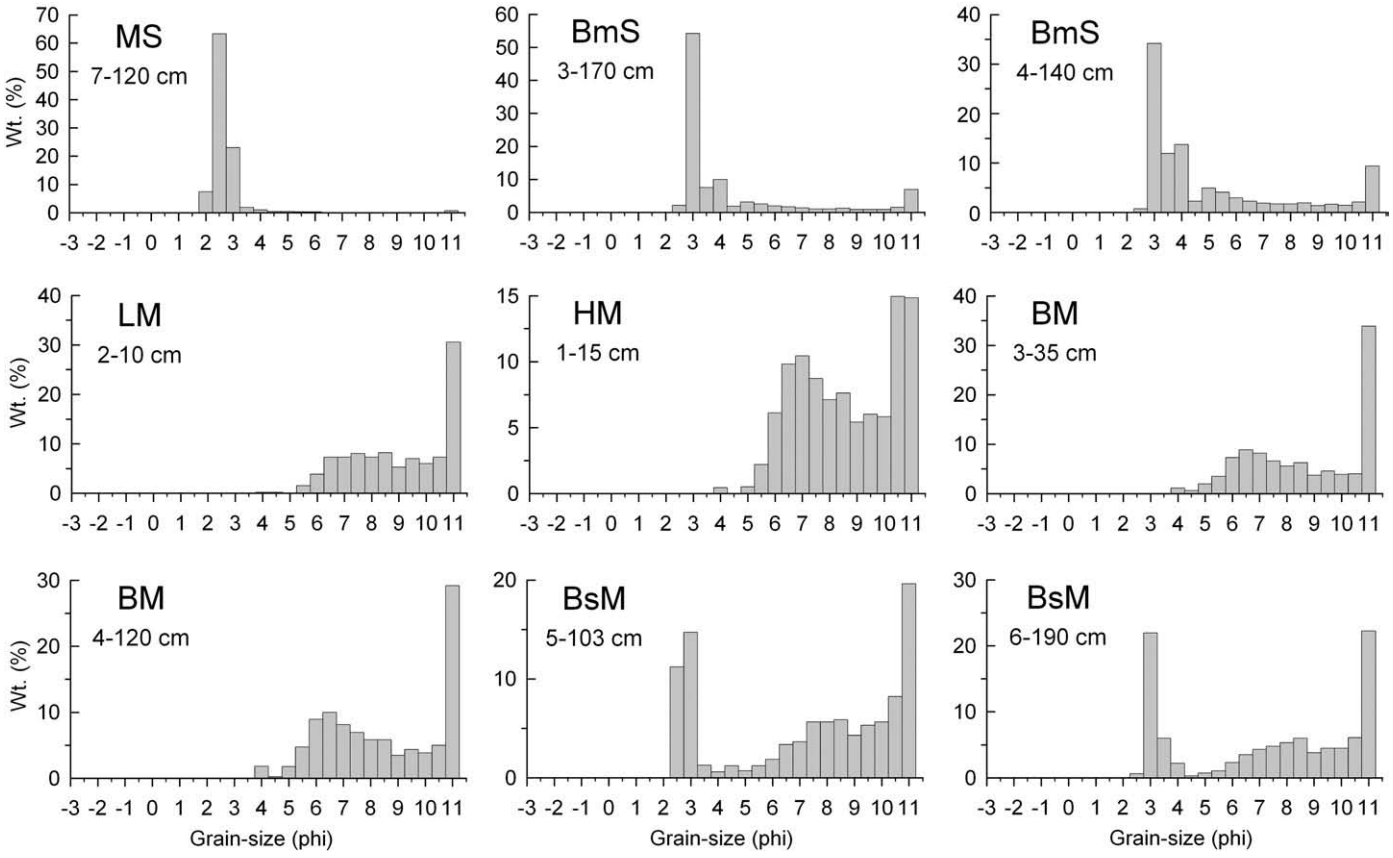

Fig. 8. Grain-size distribution of sedimentary facies. For explanation of facies codes, see the caption of Fig. 7.

(cores 2, 5 and 6) taken from the FU are dominated by bioturbated mud (facies BM and BsM) associated with laminated mud (facies LM) (Fig. 9). The area where the thin (less than 1 m thick) FU overlies the PU in the Chirp (2–7 kHz) profiles (core 3 in Fig. 5A) is characterized by the upper (ca. 116 cm thick) bioturbated/laminated mud (facies BM/LM) overlying the lower bioturbated sand (facies BmS) (Figs. 9 and 10). These lithological features suggest that the PU consists mostly of bioturbated sand (facies BmS) and the overlying FU comprises bioturbated (facies BM and BsM) and laminated (facies LM) muds. The uppermost 38-cm thick, bioturbated mud (facies BM) in core 4 (Fig. 9), corresponding to the FU, cannot be resolved in high-resolution seismic profiles due to its thin thickness (Fig. 5A). Because of the very small amount of foraminifera with rare intact shells and shell fragments in the PU consisting of bioturbated sand (facies BmS), AMS ^{14}C dating from the PU could not be analyzed. Although there are no ^{14}C ages in the PU, ten AMS ^{14}C dating from the lower–upper part of the FU (Table 1 and Fig. 9) suggests that the deposition of the PU ended prior to about 7.5 ka.

In the terraced seafloor, core sediments (cores 1 and 7) show hard, brownish sediments (facies HBS) which occur at ca. 45–193 cm below the seafloor (Fig. 9). The stiff, brownish sediments with abundant oxidized grains and cracks (Fig. 7C, D) indicate that facies HBS was formed by a pedogenic process during the period of subaerial exposure (Kim et al., 1999; Choi, 2005). The stiff brownish mud clasts in gravelly mud (facies gM) are similar in composition to the underlying facies HBS, suggesting that the mud clasts were eroded from the underlying paleosols. In core 1 where subbottom echoes are highly prolonged without the uppermost transparent layer (Fig. 5A), ca. 45-cm thick sediments of thin gravelly mud (facies gM), laminated (facies LM) and homogenous mud (facies HM) occur directly above the hard, brownish sediment (facies HBS) (Fig. 9). Where the uppermost thin (ca. 1 m thick) transparent layer is present in the Chirp (2–7 kHz) profile (core 7 in Fig. 5D), the sediments above hard, brownish sediment (facies HBS) are dominated by thick (ca. 158 cm thick) massive sand (facies MS) which corresponds to the uppermost transparent layer (Fig. 9).

5. Discussion

The elongated mound-like occurrence, the prograding inclined internal reflectors, and the most sand-sized sediments of the isolated mound can be suggestive of tidal sand ridge (Snedden and Darlrymple, 1999; Li et al., 2001; Jin et al., 2002). West and south of the study area, tidal sand ridges were extensively developed (Fig. 1A): i) Jiangsu tidal sand ridges along the Jiangsu coast (Liu et al., 1989; Li et al., 2001) and ii) East China Sea (ECS) tidal sand ridges in the submerged paleovalley of the Changjiang River (Yang and Sun, 1988; Berné et al., 2002; Chen et al., 2003). Because the study area is relatively close to these tidal sand ridges, the isolated mound can be considered as a sedimentary body related to them. The isolated mound, however, is detached from these tidal sand ridges (Fig. 1A). Furthermore, sedimentary features of the isolated mound are different from those of the Jiangsu and ECS tidal sand ridges (Table 2). The isolated mound is less elongated than these tidal sand ridges (Table 2). The isolated mound is oriented to the N–S direction, which is different from the orientation of the nearby tidal sand ridges controlled by strong tidal currents with either bi-directional or radial pattern (Table 2; Liu et al., 1989; Berné et al., 2002). The isolated mound shows symmetrical profile in transverse section (Figs. 4 and 5), whereas the Jiangsu and ECS tidal sand ridges display asymmetrical morphology in transverse section (Table 2; Yang and Sun, 1988; Liu et al., 1989; Chen et al., 2003). The Jiangsu and ECS tidal sand ridges consist of well sorted fine sand (Table 2; Yang and Sun, 1988; Liu et al., 1989; Berné et al., 2002). On the other hand, the PU of the isolated mound comprises poorly sorted muddy sand (Figs. 9 and 10). The location and sedimentary features of the isolated mound imply that there is no

Please cite this article as: Lee, S.H., et al., Depositional development of an isolated mound and adjacent area in the southern Yellow Sea during the last postglacial sea-level rise, Mar. Geol. (2009), doi:10.1016/j.margeo.2009.06.010

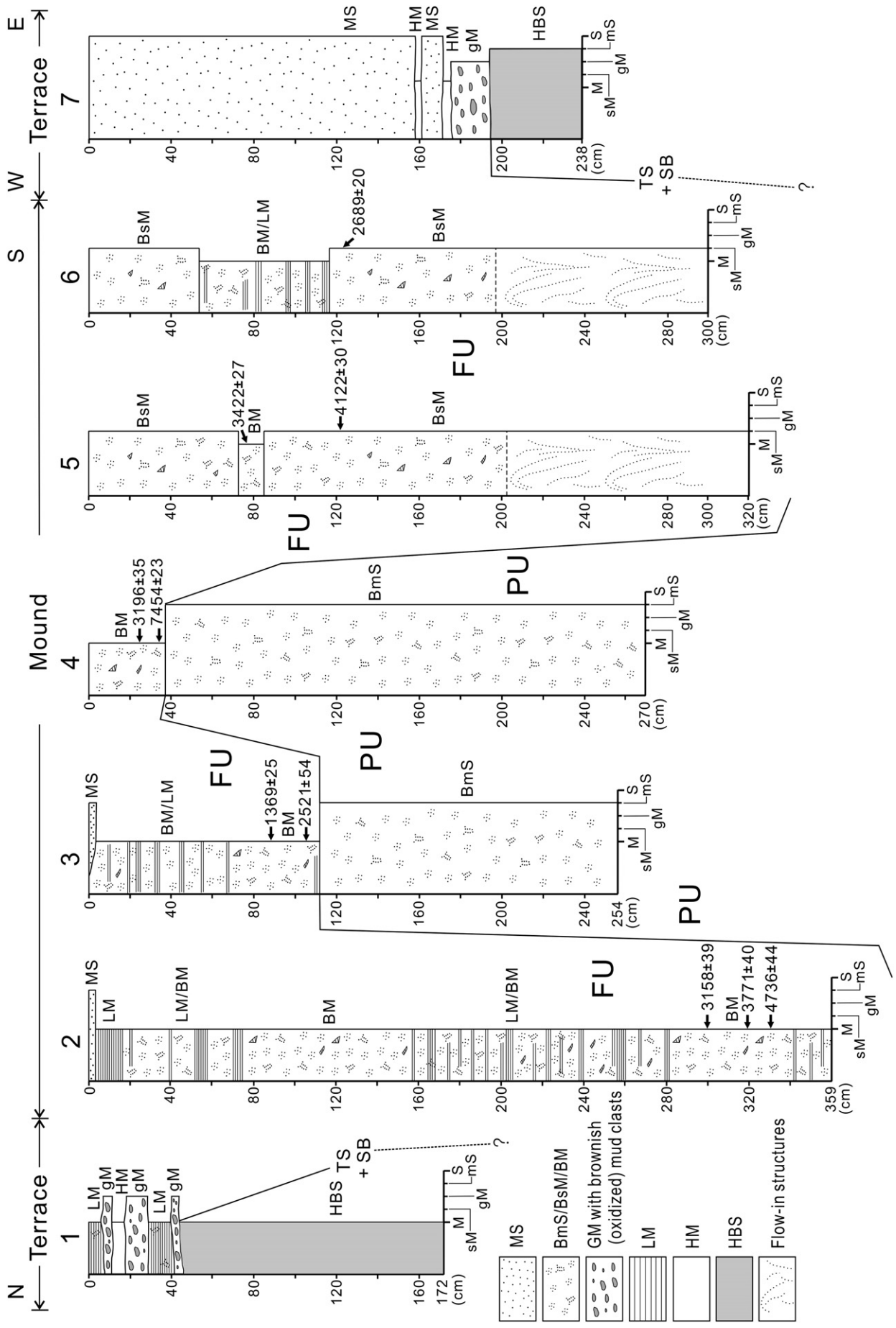

Fig. 9. Sedimentary logs of core sediments. FU = flank unit in the mound; PU = prograding unit in the mound; SB = sequence boundary; TS = transgressive surface. Facies codes on the right side of the column are explained in the caption of Fig. 7. For location of each core, see Fig. 5.

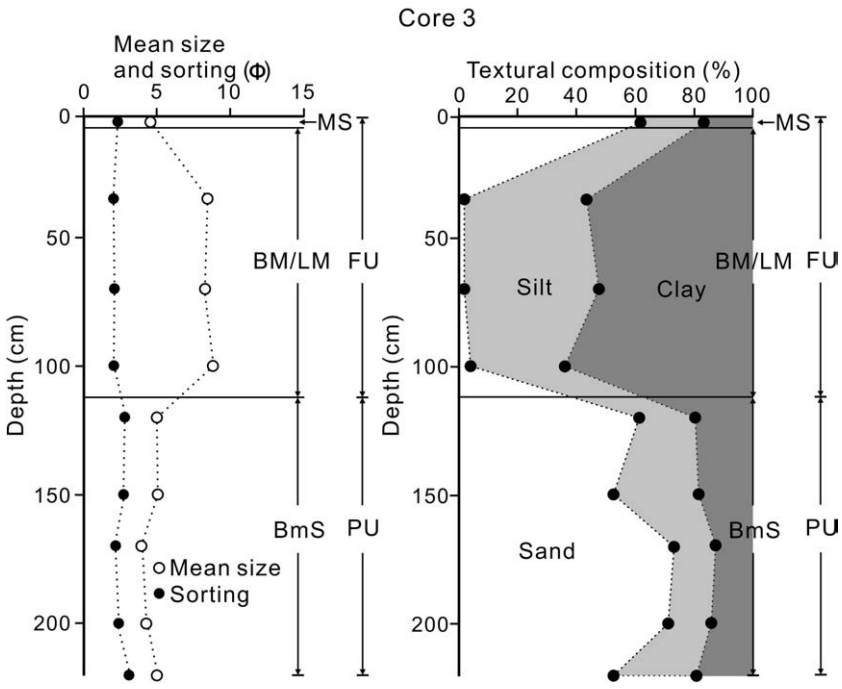

Fig. 10. Mean size, sorting and textural composition of core 3. FU = flank unit in the mound; PU = prograding unit in the mound. Facies codes are explained in the caption of Fig. 7. For location of core 3, see Fig. 5.

genetic relation between the isolated mound and the nearby tidal sand ridges.

In the terraced seafloor, the sharp, erosional boundary between the underlying paleosols (facies HBS) and the overlying gravelly mud (facies gM) with paleosol-sourced mud chips is interpreted as transgressive surface (or sequence boundary) formed by a ravinement process during shoreface retreat (Cattaneo and Steel, 2003). The very shallow (less than 0.5–2 m deep) occurrence of transgressive surface below the seafloor reflects that the terraced morphology of the present seafloor was probably attributed to stepwise topography of the transgressive surface. This terraced morphology between 50 and 60 m in water depth was most likely caused by rapid sea-level rise from −58 to −45 m during the melt water pulse (MWP) 1B around ca. 11.6 ka (Fig. 11; Fairbanks, 1989; Liu et al., 2004). The thin muddy and sandy sediments directly above the transgressive surface suggest that sediment supply into the area of terrace-like seafloor has been meager after marine transgression began at about 11.6 ka.

The intervening flat seafloor between the mound and terraced seafloor is characterized by thin (less than 1 m thick) sand veneers overlying muddy paralic deposits with a ravinement surface generated by shoreface erosion (KIGAM, 2001; Shinn et al., 2007), which is well matched with sharp surface echo and highly prolonged internal reflections in high-resolution seismic profiles. The thin (less than 1 m thick) sand veneers directly above the ravinement surface suggest that little or low amount of sediment has accumulated over the flat ravinement surface after the transgression. After the MWP-1B around 11.6 ka, rate of sea-level rise was attenuated from −45 to −36 m between 11.6 and 9.6 ka (Fig. 11). The slow rate in sea-level rise most likely produced the flat ravinement surface occurring at water depths of 43–48 m. During the late stage of this period, the nearly flat lower boundary of the PU at water depths of 37–42 m was probably generated by the ravinement process during shoreface retreat (Fig. 11).

Sea level again rose rapidly from −36 to −16 m between 9.6 and 9.1 ka, during which accommodation for deposition of the PU was probably created by the rapid sea-level rise (Fig. 11). The SSE-ward prograding internal reflectors in the PU initially developed over the small-scale convex-upward part of the lower boundary of the PU in the northernmost area of mound (Fig. 5A, C), suggesting that the small-scale mound morphology acted as a nucleus for the formation of the PU (e.g., Snedden and Darlrymple, 1999). Ten depositional ages in the lower to upper part of the FU (Fig. 9) indicate that the deposition of the PU ended prior to about 7.5 ka. The sea level rose slowly from −16 to −10 m between 9.1 and 7.5 ka (Fig. 11). Therefore, the PU is a transgressive system, most likely developed during the period of stagnation in sea-level rise between ca. 9.1 and 7.5 ka.

The isolated, elongated occurrence, the one-directional prograding nature, and the sand-sized sediments of the PU are indicative of a subaqueous relict coastal mound or wedge detached from the former proximal source area (Shinn et al., 2007). In order to maintain the consistent southeastward progradation of the PU, sandy sediments had been significantly supplied from the source area located off the northern part of the Jiangsu coast northwest of the study area (Fig. 12). Northwest of the study area, an area of sand and muddy sand occurs at water depths of 20–50 m (arrowed in Fig. 1B). This area apparently represents the erosional remnants of the early Holocene Huanghe deltaic sediments (Milliman et al., 1987, 1989; Alexander et al., 1991; Liu et al., 2002, 2004). In these previous studies about the early Holocene Huanghe deltaic sediments, there was no detailed information on size distribution, mean size, sorting, and mineralogical and geochemical compositions of surface and subsurface sediments. The

Table 2
Sedimentary features of the isolated mound, Jiangsu sand ridges and East China Sea (ECS) ridge system.

Features	Isolated mound	Jiangsu sand ridges	ECS ridge system
Dimension	40.7 km long; 29.6 km wide; slightly elongated	Tens to hundreds km long; 10–15 km wide; highly elongated	10–60 km long; 2–5 km wide; highly elongated
Orientation	N–S	Radial	NW–SE
Geometry	Symmetrical in transverse section	Asymmetrical in transverse section	Asymmetrical in transverse section
Sediments	PU: poorly sorted muddy sand	Well sorted fine sand	Well sorted fine sand
References	This study	Liu et al. (1989); Li et al. (2001)	Yang and Sun (1988); Berné et al. (2002); Chen et al. (2003)

Please cite this article as: Lee, S.H., et al., Depositional development of an isolated mound and adjacent area in the southern Yellow Sea during the last postglacial sea-level rise, Mar. Geol. (2009), doi:10.1016/j.margeo.2009.06.010

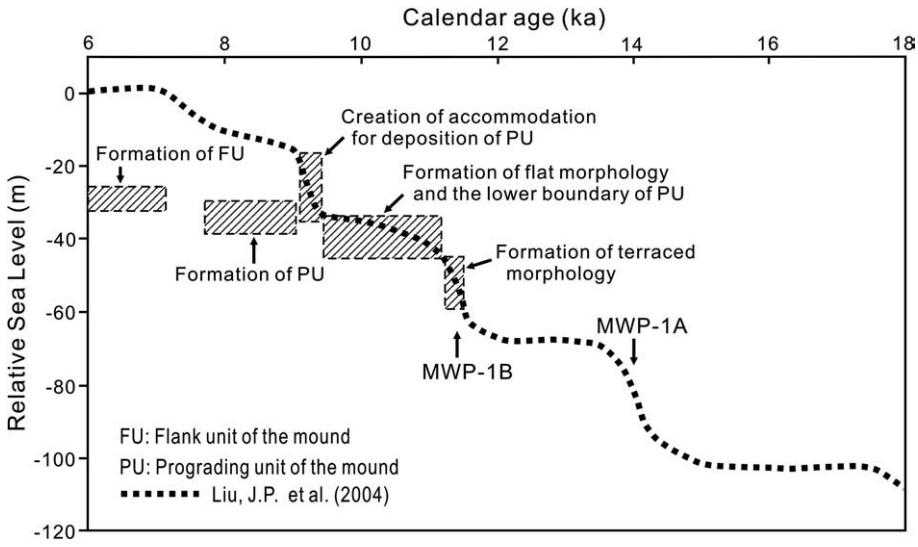

Fig. 11. Development of the mound and adjacent area related to the rate of sea-level rise during the last postglacial sea-level rise. The stripped rectangles indicate the formation age and the base-top depth range of deposits and key surfaces.

sediment properties and compositions between the PU and the early Holocene Huanghe deltaic sediments can, therefore, not be directly compared. Based on depositional timing and architecture of the Shandong mud wedge, Liu et al. (2002, 2004) suggested that extreme flooding in the middle reach of the Huanghe River at about 9 ka (Yang et al., 2000) probably caused to divert the river to the northernmost Jiangsu coast south of the Shandong Peninsula and the river apparently shifted back to the north at about 7–7.5 ka. The deposition

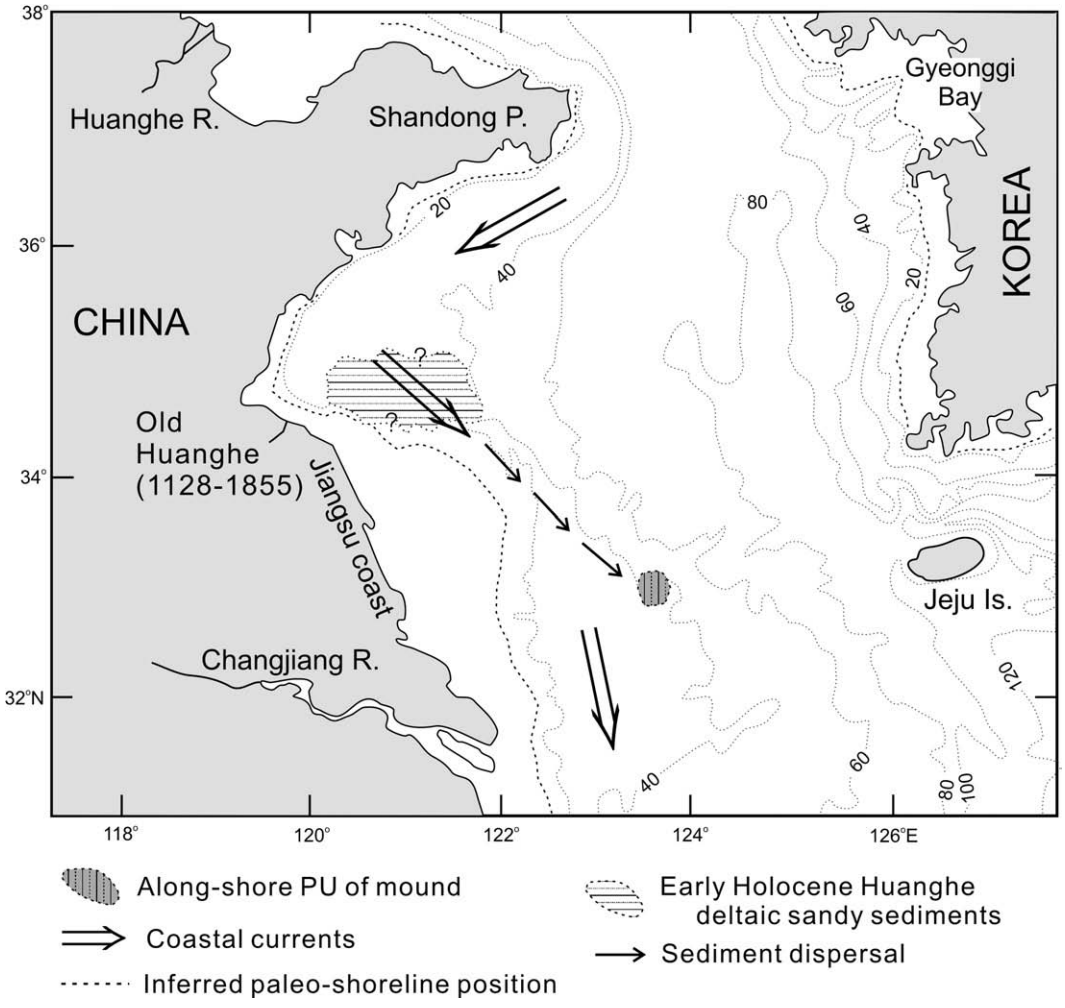

Fig. 12. Depositional model for the prograding unit (PU) in the mound formed between ca. 9.1 and 7.5 ka. Contours in meters.

Please cite this article as: Lee, S.H., et al., Depositional development of an isolated mound and adjacent area in the southern Yellow Sea during the last postglacial sea-level rise, Mar. Geol. (2009), doi:10.1016/j.margeo.2009.06.010

of the PU between ca. 9.1 and 7.5 ka is well matched with the early Holocene southward shift of the Huanghe River. Even though the direct comparison of sediment properties and compositions between the PU and the early Holocene Huanghe deltaic sediments cannot be provided, the consistent southeastward progradation of the sand-sized PU sediments, the location of the early Holocene Huanghe sandy deltaic sediments northwest of the study area, and the good match between the depositional timing of the PU and the southward shift timing of the early Holocene Huanghe River suggest that the PU sediments were presumably sourced from the early Holocene Huanghe deltaic sediments (Fig. 12).

During the formation of the PU, shoreline located between about −20 and −10 m with the NNW–SSE orientation (Fig. 12). This paleo-shoreline orientation was nearly parallel to the SSE-ward prograding direction of the PU, suggesting that the early Holocene Huanghe River deltaic sediments in the source area were probably transported or redistributed by the SSE-ward flowing coastal currents (Fig. 12). Oceanic circulation at the present time in the Yellow Sea shows the persistent southward-flowing Yellow Sea and Jiangsu coastal currents along the west coast of the Yellow Sea (Fig. 2). These coastal current systems were most likely active during the formation of the PU and had an important role on sediment transport in the Chinese coastal area at that time.

After ca. 7.5 ka, sea level rose rapidly and approached its present position (Fig. 11). Furthermore, the Huanghe River shifted back to the north and discharged directly into the Gulf of Bohai after 7.5 ka (Liu et al., 2002, 2004). The combination of the diverted river flow and rapid sea-level rise caused changes in hydrodynamic and sediment-supply regimes in the study area, resulting in the formation of highstand muddy flank unit (FU) overlying the transgressive sandy PU with a sharp, erosional surface.

Depositional development of the mound and adjacent area during the last postglacial sea-level rise indicates that transgressive and highstand deposits even within a small area were highly variable in time and space in response to changes in rate of sea-level rise, sediment supply and oceanographic regime (Figs. 11 and 12). Rapid rate of sea-level rise around 11.6 and 9.6–9.1 ka formed the terraced seafloor morphology (ca. 50–60 m water depth) and the accommodation of the PU (ca. 40–20 m water depth), respectively (Fig. 11). Spatial and temporal variations in sediment supply from adjacent coastal area associated with coastal currents resulted in the formation of thick transgressive sandy PU of the mound and thin transgressive sand sheets/veneers around the mound. The development of the PU in the mound implies that the sediment supply from the early Holocene Huanghe River south of the Shandong Peninsula strongly affected sedimentation on transgressive systems in the western part of the Yellow Sea.

Several studies including this study have suggested the early Holocene southward shift of the Huanghe River south of the Shandong Peninsula from a few indirect evidences (Milliman et al., 1987, 1989; Alexander et al., 1991; Liu et al., 2002, 2004). On the other hand, Liu et al. (2007) did not recognize the early Holocene southward shift of the Huanghe River in deep-drilling data from the Shandong mud wedge. The early Holocene southward shift of the Huanghe River is, therefore, still a controversial issue because there are still no direct evidences for the existence of the early Holocene Huanghe River delta off the northernmost Jiangsu coast. In future studies, the exact distribution, depositional timing and sediment characters of early Holocene Huanghe River deltaic sediments should be revealed in order to fully understand high-resolution sequence stratigraphic development of depositional systems in the western Yellow Sea during the Holocene transgression.

6. Conclusions

The southern Yellow Sea off the Jiangsu coastal area is characterized by an isolated mound and adjacent flat and terraced seafloor formed during the last postglacial sea-level rise. The isolated mound, 40.7 km long and 29.6 km wide, occurs above 40–50 m in water depth, and is detached from the Jiangsu and East China Sea tidal sand ridges. It consists of the SSE-ward prograding transgressive sandy unit (PU) and the overlying highstand muddy flank unit (FU) at the outer margin. The terraced seafloor occurs at water depths of 50–60 m, and comprises thin transgressive sediments overlying paleosols with a transgressive surface. The flat seafloor between the mound and terraced seafloor shows thin transgressive sands above a ravinement surface.

The terraced morphology with thin transgressive sediments was formed when sea level rose rapidly from −58 to −45 m around about 11.6 ka. As sea-level rise stagnated from −45 to −36 m between ca. 11.6 and 9.6 ka, the flat ravinement surface between the mound and terraced seafloor and the lower boundary of the PU were produced. The ensuing rapid sea-level rise from −36 to −16 m between ca. 9.6 and 9.1 ka probably created accommodation for the deposition of PU. Between ca. 9.1 and 7.5 ka, slow sea-level rise from −16 to −10 m and sediment supply from the southward shifted early Holocene Huanghe delta off the northernmost Jiangsu coast by the southward-flowing coastal currents favored the formation of the SSE-ward prograding transgressive sandy PU. After ca. 7.5 ka when sea level approached its present position and the Huanghe River shifted back to the north, the highstand muddy FU overlying the PU was deposited at the outer margin of the mound. Development of these transgressive and highstand deposits with key surfaces during the last postglacial sea-level rise was highly variable in time and space in response to changes in rate of sea-level rise accompanied with variations in sediment supply caused by the shifting of the Huanghe River.

Acknowledgements

This study was supported by the grant (PE9830S) of the Korea Ocean Research and Development Institute and the EEZ Project, Ministry of Land, Transport and Maritime Affairs. We thank the Regional Seafloor Mapping Division of the National Oceanographic Research Institute of Korea for providing Chirp subbottom profiles. We gratefully acknowledge critical and helpful comments of Prof. J. Wells (Editor) and two anonymous reviewers.

References

Alexander, C.R., DeMaster, D.J., Nittrouer, C.A., 1991. Sediment accumulation in a modern epicontinental-shelf setting: the Yellow Sea. Mar. Geol. 98, 51–72.
Beardsley, R.C., Limeburner, R., Hu, D., Le, K., Cannon, G.A., Pashinski, D.J., 1983. Structure of the Changjiang River plume in the East China Sea during June 1980. Proceedings of the International Symposium on Sedimentation on the Continental Shelf with Special Reference to the East China Sea, Hangzhou, China, vol. 1. China Ocean Press, Beijing, pp. 243–260.
Berné, S., Vagner, P., Guichard, F., Lericolais, G., Liu, Z., Trentesaux, A., Yin, P., Yi, H.I., 2002. Pleistocene forced regressions and tidal sand ridges in the East China Sea. Mar. Geol. 188, 293–315.
Bloom, A.L., Park, Y.A., 1985. Holocene sea-level history and tectonic movements. Republic of Korea. Quat. Res. Japan 24, 77–84.
Cattaneo, A., Steel, R.J., 2003. Transgressive deposits: a review of their variability. Earth-Sci. Rev. 62, 187–228.
Chen, Z., Stanley, D.J., 1998. Sea-level rise on eastern China's Yangtze delta. J. Coast. Res. 14, 360–366.
Chen, Z., Saito, Y., Hori, K., Zhao, Y., Kitamura, A., 2003. Early Holocene mud-ridge formation in the Yangtze offshore, China; a tidal-controlled estuarine pattern and sea-level implications. Mar. Geol. 198, 245–257.
Choi, B.H., 1980. A tidal model of the Yellow Sea and the Eastern China Sea. KORDI Report 80-20. Korea Ocean Research and Development Institute, Seoul. 80 pp.
Choi, K., 2005. Pedogenesis of late Quaternary deposits, northern Kyonggi Bay, Korea: implications for relative sea-level change and regional stratigraphic correlation. Palaeogeogr. Palaeoclimatolo. Palaeoecol. 220, 387–404.
Chough, S.K., Lee, H.J., Yoon, S.H., 2000. Marine Geology of Korean Seas. Elsevier, Amsterdam, 313 pp.
Chough, S.K., Kim, J.W., Lee, S.H., Shinn, Y.J., Jin, J.H., Suh, M.C., Lee, J.S., 2002. High-resolution acoustic characteristics of epicontinental sea deposits, central-eastern Yellow Sea. Mar. Geol. 188, 317–331.
Chough, S.K., Lee, H.J., Chun, S.S., Shinn, Y.J., 2004. Depositional processes of late Quaternary sediments in the Yellow Sea: a review. Geosci. J. 211–264.

Please cite this article as: Lee, S.H., et al., Depositional development of an isolated mound and adjacent area in the southern Yellow Sea during the last postglacial sea-level rise, Mar. Geol. (2009), doi:10.1016/j.margeo.2009.06.010

Fairbanks, R.G., 1989. A 17, 000-year glacio-eustatic sea-level record: influence of glacial melting rates on the Younger Dryas event and deep-ocean circulation. Nature. 342, 637–642.
Guan, B., 1994. Patterns and structures of the currents in Bohai, Huanghai and East China seas. In: Zhou, D., Liang, Y.B., Zeng, C.K. (Eds.), Oceanology of China Seas, vol. 1. Kluwer Academic Publishers, Dordrecht, pp. 17–26.
Hanebuth, T., Stattegger, K., Grootes, P.M., 2000. Rapid flooding of the Sunda Shelf: a late-glacial sea-level record. Science. 288, 1033–1035.
Hseuh, Y., 1984. The Yellow Sea circulation in winter. In: Park, Y.A., Pilkey, O.H., Kim, S.W. (Eds.), Proceedings of the Korea–U.S. Seminar and Workshop: Marine Geology and Physical Processes of the Yellow Sea. Korea Institute of Energy and Resources, pp. 86–95.
Jin, J.H., Chough, S.K., 1998. Partitioning of transgressive deposits in the southeastern Yellow Sea: a sequence stratigraphic interpretation. Mar. Geol. 149, 79–92.
Jin, J.H., Chough, S.K., 2002. Erosional shelf ridges in the mid-eastern Yellow Sea. Geo-Mar. Lett. 21, 219–225.
Jin, J.H., Chough, S.K., Ryang, W.H., 2002. Sequence aggradation and systems tracts partitioning in the mid-eastern Yellow Sea: roles of glacio-eustasy, subsidence and tidal dynamics. Mar. Geol. 184, 249–271.
KIGAM (Korea Institute of Geoscience and Mineral Resources, 2001. Study on the Marine Geology and Mineral Resources in the Yellow Sea (Yellow Sea Science Program), KIGAM Research Report (KR-01 T-07). 326 pp (in Korean with English abstract).
Kim, J.M., Kennett, J., 1998. Paleoenvironmental changes associated with the Holocene marine transgression, Yellow Sea (Hwanghae). Mar. Micropaleontol. 34, 71–89.
Kim, Y.H., Lee, H.J., Chun, S.S., Han, S.J., Chough, S.K., 1999. Holocene transgressive stratigraphy of a macrotidal flat in the southeastern Yellow Sea: Gomso Bay. Korea. J. Sediment. Res. 69, 328–337.
Larsen, L.H., Cannon, G.A., Choi, B.H., 1985. East China Sea tidal currents. Cont. Shelf Res. 4, 77–103.
LeBlanc, L.R., Panda, S., Schock, S.G., 1992. Sonar attenuation modeling for classification of marine sediments. J. Acoustic Soc. Am. 91, 116–126.
Lee, H.J., Chough, S.K., 1989. Sediment distribution, dispersal and budget in the Yellow Sea. Mar. Geol. 87, 195–205.
Lee, H.J., Chu, Y.S., 2001. Origin of inner-shelf mud deposit in the southeastern Yellow Sea: Huksan mud belt. J. Sediment. Res. 71, 144–154.
Lee, J.C., Jung, K.T., 1999. Application of eddy viscosity closure models for the M2 tide and tidal currents in the Yellow Sea and the East China Sea. Cont. Shelf Res. 19, 445–475.
Lee, H.J., Yoon, S.H., 1997. Development of stratigraphy and sediment distribution in the northeastern Yellow Sea during Holocene sea-level rise. J. Sediment. Res. 67, 341–349.
Li, C.X., Zhang, J.Q., Fan, D.D., Deng, B., 2001. Holocene regression and the tidal radial sand ridge system formation in the Jiangsu coastal zone, east China. Mar. Geol. 173, 97–120.
Liu, Z., Yichang, H., Qinian, Z., 1989. Tidal current ridges in the southwestern Yellow Sea. J. Sediment. Res. 59, 432–437.
Liu, J.P., Milliman, J.D., Gao, S., 2002. The Shandong mud wedge and post-glacial sediment accumulation in the Yellow Sea. Geo-Mar. Lett. 21, 212–218.
Liu, J.P., Milliman, J.D., Gao, S., Cheng, P., 2004. Holocene development of the Yellow River's subaqueous delta, North Yellow Sea. Mar. Geol. 209, 45–67.
Liu, J.P., Li, A.C., Xu, K.H., Velozzi, D.M., Yang, Z.S., Milliman, J.D., DeMaster, D.J., 2006. Sedimentary features of the Yangtze River-derived along-shelf clinoform deposits in the East China Sea. Cont. Shelf Res. 26, 2141–2156.
Liu, J., Saito, Y., Wang, H., Yang, Z., Nakashima, R., 2007. Sedimentary evolution of the Holocene subaqueous clinoform off the Shandong Peninsula in the Yellow Sea. Mar. Geol. 236, 165–187.
Milliman, J.D., Meade, R.H., 1983. Worldwide delivery of river sediment to the oceans. J. Geol. 91, 1–21.
Milliman, J.D., Beardsley, R.C., Yang, Z.S., Limeburner, R., 1985. Modern Huanghe-derived muds on the outer shelf of the East China Sea: identification and potential transport mechanisms. Cont. Shelf Res. 4, 175–188.
Milliman, J.D., Qin, Y.S., Ren, M.E., Saito, Y., 1987. Man's influence on the erosion and transport of sediment by Asian rivers: the Yellow River (Huanghe) example. J. Geol. 95, 751–762.
Milliman, J.D., Qin, Y., Park, Y.H., 1989. Sediments and sedimentary processes in the Yellow and East China Seas. In: Taira, A., Masuda, F. (Eds.), Sedimentary Facies in the Active Plate Margins. Terra Scientific, Tokyo, pp. 233–249.
Park, S.C., Lee, H.H., Han, H.S., Lee, G.H., Kim, D.C., Yoo, D.G., 2000. Evolution of late Quaternary mud deposits and recent sediment budget in the southeastern Yellow Sea. Mar. Geol. 170, 271–288.
Pirazzoli, P.A., 1991. World Atlas of Holocene sea-level changes. Elsevier, Amsterdam. 300 pp.
Shi, W.B., Li, D.P., Wang, X.C., Zhang, X.C., 1986. Shallow seismic surveying in south Huanghai Sea and its geological significance. Mar. Geol. Quat. Geol. 6, 87–104 (in Chinese with English abstract).
Shinn, Y.J., Chough, S.K., Kim, J.W., Woo, J.S., 2007. Development of depositional systems in the southeastern Yellow Sea during the postglacial transgression. Mar. Geol. 239, 59–82.
Snedden, J.W., Darlrymple, R.W., 1999. Modern shelf sand ridges: from historical perspective to a unified hydrodynamic and evolutionary model. In: Bergman, K.M., Snedden, J.W. (Eds.), Isolated shallow marine sand bodies: sequence stratigraphic analysis and sedimentological interpretation: Soc. Econ. Paleontol. Mineral., Spec. Publ. 64, pp. 13–28.
Stuiver, M., Reimer, P.J., Reimer, R.W., 2005. CALIB 5.0. http://www.calib.org.
Su, Y.S., Weng, X.C., 1994. Water masses in China seas. In: Zhou, D., Liang, Y.B., Zeng, C.K. (Eds.), Oceanology of China Seas, vol. 1. Kluwer Academic Publishers, Dordrecht, pp. 3–16.
Teague, W.J., Perkins, H.T., Hallock, Z.R., Jacobs, G.A., 1998. Current and tide observations in the southern Yellow Sea. J. Geophys. Res. 103, 27783–27793.
Uehara, K., Saito, Y., 2003. Late Quaternary evolution of the Yellow/East China Sea tidal regime and its impacts on sediments dispersal and seafloor morphology. Sed. Geol. 162, 25–38.
Wang, P., Zhang, J., Gao, J., 1985. A close-up view of lowered sea-level microfauna from the East China and Huanghai Seas in the Late Pleistocene. In: Wang, P. (Ed.), Marine Micropaleontology of China. China Ocean Press, Beijing, pp. 256–264.
Wells, J.T., Huh, O.K., 1984. Fall-season patterns of turbidity and sediment transport in the Korea Strait and southeastern Yellow Sea. In: Ichiye, T. (Ed.), Ocean Hydrodynamics of Japan and East China Sea. Elsevier, Amsterdam, pp. 387–397.
Yang, Z.G., 1985. The sediment and environment on the shelf of the southern Yellow Sea since the late Pleistocene. Mar. Geol. Quat. Geol. 5, 1–9 (in Chinese with English abstract).
Yang, Z.S., Liu, J.P., 2007. A unique Yellow River-derived distal subaqueous delta in the Yellow Sea. Mar. Geol. 240, 169–176.
Yang, C.H., Sun, J.S., 1988. Tidal sand ridges on the East China Sea shelf. In: De Boer, et al. (Ed.), Tide-influenced Sedimentary Environments and Facies. Reidel, Dordrecht, pp. 23–38.
Yang, D.Y., Yu, G., Xie, Y.B., Zhan, D.J., Li, Z.J., 2000. Sedimentary records of large Holocene flood from the middle reaches of the Yellow River, China. Geomorphology 33, 73–88.
Yokoyama, Y., Fifield, L.K., Lambeck, K., De Deckker, P., Johnston, P., 2000. Timing of the last glacial maximum from observed sea-level minima. Nature. 406, 713–716.

Please cite this article as: Lee, S.H., et al., Depositional development of an isolated mound and adjacent area in the southern Yellow Sea during the last postglacial sea-level rise, Mar. Geol. (2009), doi:10.1016/j.margeo.2009.06.010